Proteomic Analysis of Myogenesis: Defining The Cytoskeletome

by

Robert J. Giles

Submitted in Partial Fulfillment of the Requirements

For the Degree of

Master of Science

In the

Biological Sciences

Program

YOUNGSTOWN STATE UNVIVERSITY

ETD Program

Digitally signed by ETD Program
DN: cn=ETD Program, o=Youngstown State University, ou=School of Graduate Studies and Research, email=etdadmin@cc.ysu.edu, c=US
Date: 2013.09.04 15:10:18 -04'00'

Proteomic Analysis of Myogenesis

Robert J. Giles

I hereby release this thesis to the public. I understand that this will be made available from the OhioLINK ETD Center and the Maag Library Circulation Desk for public access. I also authorize the University or other individuals to make copies of this thesis as needed for scholarly research.

Signature:

_____

Robert Giles, Student Date:

Approvals:

_____

Dr. Gary Walker, Thesis Advisor Date:

_____

Dr. Chet Cooper, Committee Member Date:

_____

Dr. David Asch, Committee Member Date:

_____

Dr. Sal Sanders, Associate Dean, Graduate Studies Date:

Abstract

Our lab uses the C2C12 myoblastic cell line in studies of muscle development, or myogenesis. Recent studies investigated the role of the large muscle protein titin, and the small carbohydrate-binding protein galectin in myogenesis. Myogenesis requires the concerted action of a vast array of various proteins as myoblasts enter differentiation and fuse into functional muscle fibers. Our lab has hitherto lacked a full description of the proteomic changes that occur in C2C12 cells as they transit the myogenic process, especially changes that inevitably occur in the cytoskeleton and extracellular matrix as individual myoblasts fuse into extended myofibers.

This data indicates that the relative expression levels of some of the more prominent proteins change drastically during this process, by comparing densitometry data from cellular lysate samples extracted from cell lines at regular intervals from differentiating myoblasts. The investigation also demonstrates the possibility post-translational modifications occurring in various low molecular weight proteins made apparent by gradual electrophoretic mobility shifts of specific bands throughout the time course.

This investigation allows this laboratory's studies to proceed into more detailed investigations of myogenesis, particularly morphological and proteomic changes that occur when C2C12 myoblasts are cultured upon fascia tissue. One dimensional electrophoretic analysis is insufficient to fully account for the complete changes that occur in the proteome of C2C12 myoblasts. Therefore, future work should include two dimensional SDS-PAGE to gain a better appreciation for the changes that occur in a proteome.

Acknowledgements

It seems it has been a long journey to get to this point, and it would take a very long list of to name all the people have helped in some way to achieve this, This work could easily double in length if I were to compose a complete list. Nevertheless, none of these people are more important than my family. I owe countless thanks to my parents Richard and Teresa Giles for encouraging me always try and always carry on. I will always regard my brothers Richard and Michael as my best friends, whom were a constant influence on myself, and afforded me the motivation to always aim to improve myself.

I joined Dr. Walker's lab sometime in the spring of 2009, about four and a half years ago. I remember spending what seemed like eternities watching buffer wash through the affinity chromatography column (I think it required four washes). It never really mattered how long it was because I genuinely enjoyed spending time in the laboratory, learning about laboratory procedures, and acquiring a new, large second family, in what I considered to be my second home. For this, I must express my sincere gratitude to Dr. Gary Walker who over these past years provided me with great advice, patience, and optimism. Dr. Chet Cooper provided me with significant opportunities during my tenure here, which allowed me to spend more time to participate and gain experience in the laboratory. I also must express my gratitude to Dr. David Asch and Dr. Jonathan Caguiat, who likewise, have been very helpful and generous with their time towards me.

I consider my fellow graduate students in the laboratory to be my second family, and I could not imagine doing this without them must thank Lisa Boyer for being a mentor to me, and giving a solid background that made this research possible. I must also thank

Sumedha Sethi for answering endless questions when Lisa was not around, or when Dr. Walker was busy. Stephanie McCann and Steve Robbins also have my thanks for me the ropes of mammalian cell culturing. I have great respect for all of my peers. Aaron, Suzie, Valentine, Beatrice, Noina, Evelyn, Mike and Dana have been wonderful friends and invaluable allies during my time here. I wish them all the best.

Table of Contents

List of Figures

List of Tables

1. Introduction

1.1 Myogenesis

The process of muscle development, or myogenesis is an intricate process, from the initial differentiation of the embryonic stem cell to the cellular fusion of mature myocytes to formation of a highly specialized myotube. The specific processes underlying myogenic differentiation have steadily been the subject of study for over one hundred years, but the greatest progress has only been made in the preceding two decades, due to advances in contemporary experimental techniques. This has led to a broader understanding of myogenic regulation on the transcriptional level, early in differentiation (Thorsteindóttir, 2011).

When myoblasts exit the cell cycle and begin to mature, a very precise organizational process must occur in order to produce functional muscle tissue. A vast multitude of proteins with varied functions that must be set into place in a coordinated manner as individual myoblasts fuse into elongated myofibers, and the construction of the fundamental contractile apparatus of the myofiber, the sarcomere, begins to occur. There is much that still needs to be resolved to this end, as many of the more complex aspects of the organization process remain nebulous. Such intricacies are critical to gaining a full appreciation of the process. If even subtle irregularities in protein expression occur, the entire system can become jeopardized.

One important area of study has been of the large filamentous proteins that span the sarcomere. Although initially thought to be simply structural features, it is now thought

that these proteins have critical roles in sarcomerogenesis. It has been suggested that portions of these long proteins serve as templates for sarcomere assembly. The proteins bind many different molecules, including scaffolding and regulatory proteins. It is therefore thought that sarcomere formation occurs in multiple iterations with these large proteins placing each component of the sarcomere in a successive manner (Kontrogianni-Konstantopoulos, 2009).

Because myoblasts begin as individual cells and must eventually become a multinucleate syncytium, the cytoskeleton must be remodeled significantly to accommodate such widespread changes. Understanding how global changes in the cytoskeletal proteome relates to the proteomic changes of the sarcomere and internal environment in general can serve to help clarify the understanding of the proteome, opening the door to deeper studies into myoblastic proteome.

1.2 The Sarcomere

The sarcomere is a repetitive apparatus that maintains a rather recognizable appearance of regular dark and light bands when observed through light microscopy. This is because sarcomere is packed with variously functioning proteins, and their density varies throughout the length of an individual sarcomere. The distinctive banding pattern is the basis for the nomenclature associated with sarcomere structure. There are three bands apparent within the sarcomere which are termed A, I and Z. The A-bands are particularly wide and contain one of the major contractile components of the sarcomere, the so-called thick filament, myosin. In between two A-bands is the darker, much thinner M-line. The A bands are flanked by I bands which include the other contractile component, thin

filament actin. The band that appears the darkest is that which forms the edges of a sarcomere. This is the Z-band (or Z-disc) and it contains the greatest density of sarcomeric proteins. It acts mainly as a scaffold that supports the contractile apparatus formed by actin and myosin and their associated proteins (Sanger, 2008).

The two major components of a sarcomere are referred to as the thick filament and the thin filament. The thick filament consists of the motor protein myosin. Myosin has characteristic “head” domains which, during muscle contraction, bind the thin filament. The thin filament is made up of actin, tropomyosin, and troponin molecules. These proteins work in concert to produce the “power-stroke” that drives muscle contraction as per the sliding filament model. In addition to the thick and thin filaments, there are three other very large, filamentous proteins that seem to have important support roles in muscle contraction.

These are the “giant” filamentous sarcomere proteins: nebulin, obscurin and titin. Nebulin binds actin in striated muscle, and produces muscle contraction by interacting with the α-actin that constitutes the I-band, and nebulin. It extends concurrent with actin, with its N-terminus aligned with the ends of the thin filaments, and its c-terminus is anchored to the Z-disc. Obscurin is a multidomain, albeit linear protein composed of adhesion modules and signaling domains. It is not included in the sarcomere proper, but exists on its peripheries. Titin is the most abundant of these three, and in general the third most common protein in the sarcomere, behind only actin and myosin. Moreover, titin is the largest protein in the sarcomere; a single titin molecule spans half the sarcomere’s length, with its N-terminus anchored to the Z-disc, and the C-terminus in the M-band. It is for this reason that titin is thought of as the sarcomere’s third filamentous system,

along with actin and myosin (Kontrogianni-Konstantopoulos, 2009). Titin, due to previous investigations done in this lab, is of particular interest in this research, and is discussed in detail further on.

1.3 The Cytoskeleton and Transmembrane Proteins

All cells, irrespective of their nature, contain a support system in the cytoplasm referred to as a cytoskeleton. In eukaryotes, the cytoskeleton serves a few important functions outside of helping a cell maintain its shape. The cytoskeleton also serves to provide feedback from the external environment. It affords a cell to changed shape, which is an utter necessity in the somewhat unique scenario presented by myogenic process, as myotube formation would require frequent remodeling of the cytoskeleton in order to accomidate syncytium formation. Given these things, differential expression, especially within the context of the interconnectedness of the system as a whole, can shed light on what future investigations may be appropriate.

Cytoskeleton architecture is based on three types of filamentous systems. The smallest are microfilaments which are made up of another form of the often encountered protein actin, than that which is found in the sarcomere. Intermediate filaments are derived from several types of fibrous proteins, and are generally more robust than microfilaments, although they perform similar functions of structural support. Microtubules are cylindrical complexes of the fibrous protein tubulin, and have additional rolls in intracellular transport. Transmembrane proteins such as integrins have been shown recently to have important roles in myoblast differentiation (Przewozniak, 2012). Such

proteins are important for myoblast's ability to adhere and fuse into myotubes, and changes in their expression could be encountered in future studies.

1.4 The Myogenic Factors during Myogenesis

Changes in the expression of all of the aforementioned large proteins would be the result of the action of a vast array secreted transcription factors, which themselves are likely the conclusion of lengthy signaling cascades based on the action of many different kinases and other small proteins. The myoblasts, as used in this research, require s supplement of serum in order to proliferate. This is because the serum contains a host of growth factors that *in vivo*, would be secreted from outside the cell.

It is understood that in the vertebrate embryo, the somite divides in a progressive manner, first into two subdivisions, the dermomyotome, and sclerotome, which will eventually form the vertebrae and ribs, the dermomyotome, further divides dermatome and the myotome as development progresses. This division produces dermis and muscles of the trunk, respectively. The myotome is the developmental progenitor of skeletal muscle tissue, but the cells at this point are not truly myoblasts. At this stage of development, all muscle precursor cells express the transcription factor *Pax3*. After the commencement of myogenesis, the expression of *Pax3* decreases, and expression of specific myogenic genes begins to occur in a phased manner that corresponds to the many stages of myoblast differentiation. These are the critical components in the regulation of myogenesis, a group of basic helix-loop-helix proteins referred to as myogenic regulatory factors (MRFs) (Yokoyama, 2011).

It is the MRFs that oversee the commitment of myoblasts and their subsequent differentiation. As the principal regulatory factors of skeletal myogenesis, tight control of the process depends on the concerted interaction of MRFs. It is also understood how MRFs are in part governed by growth factor signaling, which either act to promote or inhibit myocyte growth, but it is still unclear precisely how differentiation progresses and it remains an active center of study (Thorsteindóttir, 2011). Although the MRF's are the critical regulatory proteins of myogenesis, their activity is dependent on the complex signal transduction system that includes perhaps most importantly the various kinases that are collectively called the myogenic kinome.

Amongst the pertinent kinase proteins are the extracellular-signal regulated kinases (ERKs) are also referred to by the name MAPK for *mitogen-activated kinase* or MAP2K for *microtubule-associated 2 kinase* in older literature. The general name ERK generally applies to two isoforms, ERK1 and ERK2. Nevertheless, ERK is stimulated by a variety of growth factors and mitogens (hence the alternative name). The expression of ERK is unique in myocytes, where expression occurs in a biphasic manner. (Knight 6-8) The ERK pathway is active during the proliferation phase, and represses transcription of genes required to commence differentiation. ERK activity decreases as cells become ready to differentiate. Once differentiation is initiated, and myogenesis is actively occurring, ERK activity again increases, being a required component in the differentiation. Therefore, ERK seems to be a dual-function kinase with respect to myogenic differentiation, it has inhibitory roles in the early stages, and stimulatory roles in the later stages (Tagawa, 2008). Close relatives of the ERKs are the p38 family of kinases. These are also referred to as MAPK proteins, and there are four known isoforms,

but only one, p38α, has been shown to be critical to cell differentiation. Studies done both *in vitro* and *in vivo* demonstrated that p38α is indeed a necessary factor in myoblast differentiation, however other studies have shown that it is not induced in the somites during embryonic development. (Knight, 2011) Another important kinase, Akt first came to light as the product of an oncogenic v-akt of the mouse retrovirus Akt8. One of the major targets of Akt as a kinase is the mammalian target of rapamycin (mTOR).

When the complex signaling cascades cause the immature cell to begin to express MRFs, it will either migrate from the somite to form distal muscles or remain in the somite and form the muscles of the trunk. (Deries, 2012). Regardless, the cell can then be described as being a myoblast. Myoblasts soon thereafter develop an elongated morphology, and fuse into myotubes, and eventually mature muscle fibers (Yokoyama, 2011). The adult muscle fiber is formed from two distinct components, the myofibrils, and their membrane binding along with its associated structural components. When muscle cells begin to differentiate, they begin to express the required proteins for the myofibril to form, leading to the development of the sarcomere.

1.5 Galectin-1

Galectins are a class of the carbohydrate-binding proteins, lectins, which bind β-galactoside sugars specifically. Galectins participate in a wide variety of processes including interaction of the extracellular matrix as well as cellular proliferation and apoptosis. One member in particular the different members of the galectin family, galectin-1 has been implicated in important roles of myogenesis, and for this reason, is of

particular interest to this laboratory's ongoing research. Galectin-1 is conceivably expressed in all mammalian tissue types.

There are several lines of evidence that suggest that galectin-1 has a critical role in skeletal myogenesis In skeletal muscle, galectin-1 is localized to the sarcoplasm prior to differentiation, when the myoblasts are still in their mononuclear state, but migrates to the extracellular regions as the cells begin to fuse into myotubes. This migration and the presence of the protein in skeletal tissue in general is intriguing. It has been shown early on the galectin-1 has an antagonistic relationship with the integrin α7β1, myoblasts' major receptor of laminin. Because increased expression of α7β1 has been shown to prevent the onset of muscular dystrophy, and since integrins are important in regards to cytoskeletal remodeling during differentiation, it seems that galaectin-1 may have an important role in the differentiation process. This is corroborated by the revelation that galectin-1 expression is highest at the same time that myoblast fusion is occurring at its maximum rate. Moreover, fibroblasts will convert to muscle cells in culture, upon introduction of galectin (Georgiadas, 2007).

Despite what is suggested by *in vitro* studies, galectin-1 null mice have no obvious phenotype, and any abnormalities are modest and often observed in the nervous system. The single most important finding with respect to the myogenic process in galectin-1 null mice is that they seem to have some degree of attenuation or delay in their ability to regenerate muscle fibers (Georgiadas, 2007). Because myofiber formation is diminished after trauma, it is suggested that galectin-1 may act in the same pathway that lead to expression of certain MRFs such as MyoD, myogenin and My5.

1.6 Titin

One of the most abundant protein components of the sarcomere is the giant fibrous protein titin. The structure of titin is separated into two sections, that which spans the I-band (the end connected to Z-disc) and that which span the A-band (which runs parallel with actin). Titin is often divided in this way because the structure changes drastically at the I/A boundary (Krüger, 2011). In the A-band, titin is dominated by a lengthy, repeating pattern of about 300 of the same two protein domains, fibronectin type-III (Fn-III) domains and immunoglobulin (Ig) domains, and a kinase domain near the c-terminus in the area that spans the M-band. Interestingly, this super-repeat region is conserved in such a way similar to actin. Furthermore, the periodicity of the Fn-III and Ig domains complements closely actin, which is thought to allow for titin's binding to the thick filament. (Tskhovrebova, 2010) The I-band portion consists primarily of the same type of Ig domains linked in tandem, save for the appearance of a motif with a high incidence of Proline (P), Glutamate (E), Valine (V), and Lysine (K) residues in the amino acid sequence. Because of this, such a motif is referred to as PEVK (Kontrogianni-Konstantopoulos, 2009).

Titin is encoded by a single gene, *TTN*, that is, in the case of mice and human genomes, located on the long arm of chromosome 2. (Kontrogianni-Konstantopoulos, 2009). The mRNA of *TTN* is subject to differential splicing, leading to the presence of plausibly millions of different isoforms (9905). The presence of titin isoforms was first suggested when variances in the electrophoretic mobility of titin were detected in samples extracted

from different tissue types. This was confirmed when the structure of titin was determined in the late 1990s. Different titin samples exhibited three unique electrophoretic bands. (Vikhlyantsev, 2006) The three major isoform groups were established and named N2A, N2B, and N2BA. Titin with the N2A domain is expressed in all skeletal muscle and occasionally in cardiac muscle, whereas titin with the N2B domain is found exclusively in titin expressed in cardiac muscle. Titin N2BA shares structural components of both N2A and N2B and is also found exclusively in cardiac muscle (Kontrogianni-Konstantopoulos, 2009). The splice factors that generate the various isoforms are largely unknown, although a recent article identified the cardiomyopathy gene RBM20 as regulator of titin's splicing (Guo, 2012).

Although titin is found in cell types other than myocytes, muscle function roles for titin have been elucidated. The first role of titin to be suggested was based on the regularity of the super-repeat component with respect to the thick filament. It is thought that titin acts as in some capacity as a sarcomeric measuring stick while the thick filament is being set-up during the organization of the sarcomere. Another proposed role for titin is related to the presence of titin's Ig-tandem repeats, PEVK and the N2B variable region in the I-band. These components allow titin to be functionally elastic and extensible, and unravel when the sarcomere stretches, and contribute to about half of the tension exhibited by muscle when it is relaxed. The degree of tension is modified by switching the isoform being expressed. In cardiac muscle, the N2BA/N2B ratio decreases during development, and this effects a greater degree of tension; during incidences of chronic heart failure, the N2BA/N2B ratio increases, and the tension becomes less. (Krüger, 2011)

Titin is an important signaling node. Phosphorylation sites are present throughout the length of titin, and the N-terminal region of titin, inside the Z-disc, contains two sequence insertions that encode kinase domains that, in vitro, were demonstrated to be phosphorylated by ERKs. Similar phosphorylation motifs were observed at the opposite end of titin. Phosphorylation may be important during myogenesis, for the proper alignment of titin during its integration into the sarcomere. Titin has been shown to interact with over twenty different proteins, many of which are located in the densely packed z-band. A particularly strong interaction occurs between the z-band protein telethonin, alternatively called the T-cap, and the z-band region of titin. A ligand of telethonin is the transcriptional coactivator muscle LIM. These three are thought to constitute a sarcomeric mechanosensor complex, but the true nature of this apparatus remains nebulous (Krüger, 2011).

Calcium has been shown to be an important binding partner of titin. The stiffness of PEVK and the other extensible regions of titin are modulated by the concentration of Ca^{2+}. (Nocella 2012) Moreover, Ca^{2+} has been shown to regulate titin's placement during sarcomerogenesis, and when Ca^{2+} transients are blocked, the arrangement of myosin and actin is compromised. The C-terminal kinase domain of titin requires activation by Ca^{2+}. Since this kinase domain has been shown to initially subside in the forming z-band during sarcomerogenesis, it has been proposed that titin's associations with the thin filament are dependent on Ca^{2+} transients (Harris, 2005).

1.7 Autoimmune Rippling Muscle Disease

In the sarcolemma, like the membranes of other cell types, there exist deep invaginations referred to as caveolae, whose structure is maintained by small transmembrane proteins called caveolins. In mature muscle fibers caveolins are also found in the T-tubules, where ion channels, membrane pumps and various kinases gather. Caveolin-3 (CAV3) is an isoform specific to muscle cells. In addition to its function as a converging center for proteins, it has roles in myoblast differentiation and fusion, and its transcription increases over the course of differentiation. Mutations in the gene CAV3 have been linked to such diseases as muscular dystrophy. Another disease that is linked to mutations in CAV3 is rippling muscle disease (RMD). (Ullrich, 2010). RMD is characterized by percussion-induced muscle mounding, generating a visible rippling effect across the length of a muscle. The contractions are electrically silent; they occur without any incidence of a motor unit action potential. Though the precise role of CAV3 in diseases such as RMD and myofiber physiology in general, is not well understood, CAV3 mutations affect the function of DHPRs. Also, CAV3 has also been shown to associate with the ryanodine receptor (RyR1), a calcium release channel of the sarcoplasmic reticulum. It is therefore thought that CAV3 has an important role in the maintenance calcium homeostasis.

In 1996, a myasthenia gravis (MG) patient showed symptoms similar to that of RMD. MG is an autoimmune disease caused by a disruption of transmission at the neuromuscular junction. In the majority of patients the disruption is caused by antibodies to the acetylcholine receptors in the sarcolemma (Walker, 1999). Some other patients that do not have antibodies to acetylcholine receptors have been shown to exhibit antibodies to a tyrosine kinase specific to muscle. Since the immunosuppressive treatment typically

applied to MG patients also alleviated these symptoms, it was believed that the cause of the rippling muscles in this case was also autoimmunity. Furthermore, because the rippling was brought on by percussion as in genetically linked RMD, it is thought that mechanosensitive ion channels are the core root of the symptoms in autoimmune rippling muscle disease (ARMD). Sera was obtained from ARMD patients and used to immunoscreen a human skeletal muscle cDNA library to identify possible antigens in the disease. Some of the antigens identified were located on the N2A isoform of titin, in two main regions. One is in a region of A-band titin near PEVK, close to, but separate from, the main immunogenic region (MIR) that is associated with MG. The other is in the I band titin not far from where the A/I boundary is located (Watkins, 2006). Since the later antigenic region of titin appeared to be specific for ARMD it was therefore subjected to further study. Sequence analysis indicated that the region is encoded on exons 248-250 of TTN (Zelinka, 2011). It was this line of research in our laboratory that lead to interest in titin, and, eventually, myogenesis in general.

1.8 Specific Aims

The goal of this research is to outline the dynamics of the protein profile of C2C12 myoblasts as they transit the myogenic process during the course of differentiation. These investigations will help facilitate future investigations of more particular aspects of the myoblast proteome with respect to the myogenic process. We hypothesize that the proteome and composition of the cytoskeleton will change during myogenesis.

2. Methods

2.1 Mammalian Cell Cultures

Culturing of C2C12 myoblasts proceeds using media which incorporates Delbecco's modification of Eagle's media (DMEM) supplemented with varying amounts fetal bovine serum (FBS) and a constant 1% concentration of Penicillin-Streptomycin solution (PS). DMEM contains essential nutrients for cell growth, whereas FBS contains the key growth factors that signal cells to divide. PS functions as an antibiotic/antimycotic to stem the likelihood of contamination of the cultures, which has been shown to be a persistent problem. Three different solutions were used: C2C12 Initial Growth Media (C2IGM) is by volume ~20% FBS, which hastens the growth process in newly started cultures. C2C12 Growth Media (C2GM) is by volume ~10% FBS, and C2C12 Differentiation Media is by volume only ~1% FBS. This low concentration of signaling proteins leads to a shift from proliferation to differentiation into mature myofibers.

Myoblasts were purchased from ATCC in frozen 1 ml tubes and stored in liquid nitrogen until culturing was ready to proceed. Cells were thawed rapidly to 37°C in a water bath and mixed with 37°C C2IGM in a gradual, stepwise manner, mixing the thawed culture 1 ml with an equal volume of media in fifteen ml conical centrifuge tube, followed by 2 minutes of incubation at room temperate, which is then proceeded by another addition of an equal volume of media. After another 2 min. incubation, six ml of C2IGM was added to produce a final volume of 10 ml. The culture was then transferred to a $75cm^3$ canted-neck culturing flask. An additional 10 ml are added to the flask to produce the final volume of 20 ml. The culture was incubated at 37°C with 5% CO_2. Within 24 h,

myoblasts will have attached themselves to the bottom of the flask, allowing for media to be refreshed without disturbing the cells themselves. Since the particular mixture of DMEM used for this procedure contains a pH indicator, a red color shift in the normally pink media indicates that the pH has shifted due to cellular metabolism and requires replacement.

After two days. C2IGM was replaced with C2GM and cultures were grown to between 80% to 90% confluency. At this point the cells were trypsinized. In this, media is removed and 10.5 µL of 37°C trypsin is added to loosen the cells' attachment to the flask) and 0.5 µL was aloquated into 21 new $25cm^3$ canted-neck culturing flasks, and 19.5 ml of 37°C C2GM was added. Cultures were again grown to 80% to 90% confluency, at which time, C2GM was replaced with C2DM in 18 of the 21 cultures, whereas 3 of the cultures were harvested immediately. Other groups of three cultures were harvested after 24 h, 48 h, 96 h, 144 h, 192 h, and 288 h. This produces a time course with seven time points, each in triplicate.

2.2 Preparation of Samples

Cell cultures from the first time course were harvested using Qiagen RNeasy Mini Kit, according to the manufacturer's protocol via in-flask lysis, after being washed with DMEM. During this procedure, the whole cell lysate (WCL) from the first flow through was conserved. Protein was precipitated with six volumes of -20°C acetone. The samples were allowed to precipitate overnight at 4°C. The next day, samples centrifuged, and the acetone supernatant was removed, and the pellet was washed once with cold acetone for

five minute at ~38×g. Proteins were solubilized using protein solubilization solution (PSS) and stored at -20°C

Cell cultures from the second time course were harvested with a Triton X-100 protein extraction. This method allows the sample to be divided into portions based upon their solubility in the detergent Triton X-100. Cultures were first washed with DMEM, and again with 1 ml of isotonic Wash Buffer and then treated with 1 ml of a buffer containing Triton X-100, by gentle rocking while on ice for 5 min. The buffer, now bearing detergent soluble proteins, was transferred into 1.5 ml microcentrifuge tubes and stored at -80°C. At a later time, the proteins of the detergent-soluble portion (DSP) were precipitated from the buffer using -20°C acetone following the same procedure described above. The cultures were than washed again with 1 ml of tris buffer, and the cells were lysed by jetting 1 ml of 1X SDS sample buffer over the cells repeatedly until the membrane has dissolved completely. The lysate, which contains the detergent-insoluble portion of proteins (DSP) was frozen at -80°C for later analysis.

2.3 Gel Electrophoresis

For the WCL acquired from the first time course, 15 µL of the WCL protein was mixed with 5 µL of 4X SDS sample buffer, and loaded onto a Bio-Rad Criterion TGX 8-16% 1mm precast gel. The gel was run with tris-glycine-SDS (TGS) running buffer at a constant 100 V for ~1 h and 40 min. For the detergent-soluble portion (DIP) acquired from the second time course, 20 µL of the lysate was loaded onto a Bio-Rad Criterion TGX 8-16% 1mm precast gel, and ran using the same conditions as described above. For the detergent-insoluble portion (DSP) acquired from the second time course, 20 µL of the

lysate was loaded onto a Bio-Rad Criterion TGX 8-16% 1mm precast gel, and ran using the same conditions as described above.

2.4 Gel Analysis

All gels were stained using one of two methods. Coomassie stain was applied to a gel while shaking for no less than 1 h. Two destains, the latter being simply more dilute, were used in sequence to destain the gel. The first, "high destain" was applied to the gel for 1 h, or until the stained gel became translucent again. The second "low destain" was applied until the gel was completely or nearly clear, and the bands were easily differentiable from the background stain. Sypro Ruby Red is a fluorescent stain manufactured by Bio-Rad, seems to produce results better suited for densitometry of a complex profile such as the C2C12 WCL. This process utilizes the high destain used in the coomassie destaining as a fixing solution, inhibiting the migration of the proteins from the gel during the Sypro staining process. The fixing solution was applied for 1 h, while shaking after being replaced by Sypro Ruby Red overnight.

After either staining/destaining process was complete, the gel was scanned into a computer using the Pharos FX system from Bio-Rad. The image produced can be viewed using the Quantity One program, also from Bio-Rad. The image can be transformed to enhance the visual qualities of the image, such as brightness and contrast, and background elimination. These alterations have no bearing on the actual data represented in the image, and serve only as visual enhancements for the viewer. When lanes are established over the image, background was removed from the densitometry plot, which does alter the actual data. After this, bands of interest were selected and their

corresponding densitometry was compared across various the seven time points. In addition changes in the profiles of both the DSP and DIP were compared across the seven time points. With respect to the WCL sample, the densitometries of high molecular weight proteins were compared with that of low molecular weight proteins. If BSA standards were loaded onto the gel, it was possible to establish a standard curve and extrapolate quantity to the protein in a particular band or set of bands.

2.5 LC-MS-MS Analysis

In order to identify the protein content in specific bands of the DIP samples,three individual bands and one doublet of bands (Fig. 1) were excised from a Coomassie-stained gel and submerged in 5% v/v acetic acid, and frozen at 20°C for further analysis. The four samples were submitted to Ohio State University Mass Spectrometry and Proteomics Facility, where the proteins were partially sequenced via Capillary-liquid chromatogragraphy-nanospray tandem Mass Spectroscopy (LC-MS-MS). Partial sequences were search against the UniProtKB/Swiss-Prot protein database, and the resulting scores and identities were returned.

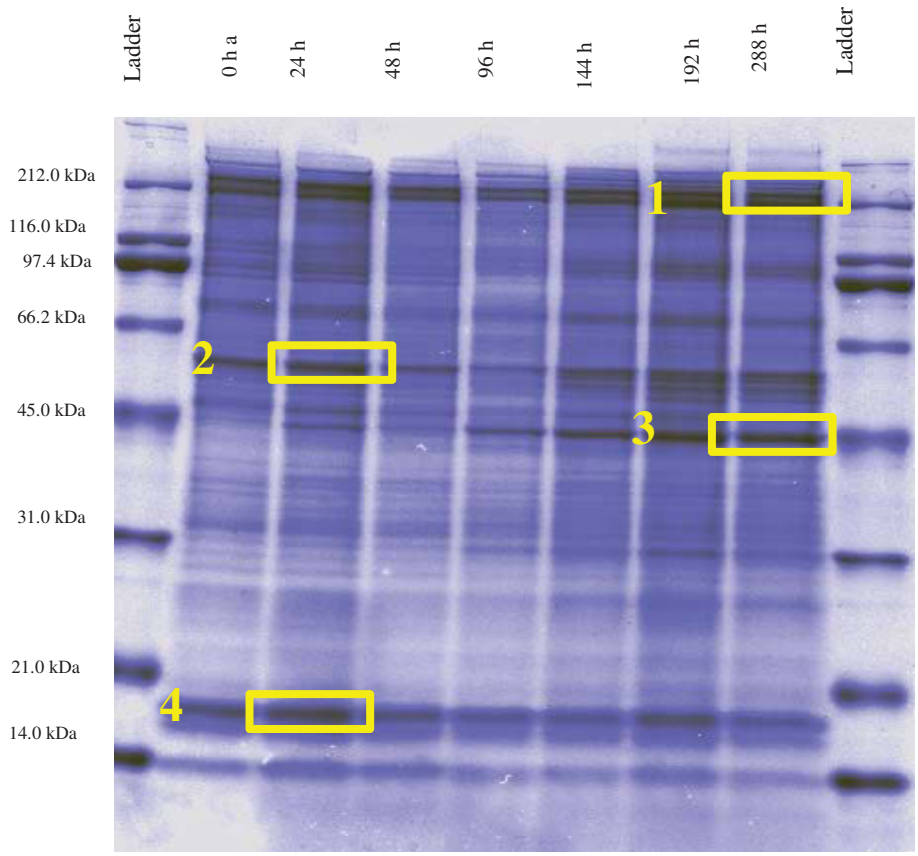

Fig. 1. Electrophoretogram of the detergent insoluble portion (DIP). Bands excised for LS-MS-MS analysis are indicated by yellow boxes

3. Results

3.1 Introduction

All gels were analyzed using the *Quantity One* software from Bio-Rad. The initial time course produced samples consisting of the whole cell lysate (WCL). Since this sample is relatively complex, the analysis consisted of densitometry of 10 protein bands visible at all time points, based on the molecular weights provided by broad range molecular weight standards ran concurrently with the samples. Two related measures of densitometry were used, the average band density and trace density. Trace density measures the entire area under the curve of the band's densitometry plot. Band densities in a 1-dimensional electrophoretogram generally have a Gaussian shape. This is to say that the density is low at the peripheries of a given band and highest in the center. However, two bands with equal trace density can have unique band morphologies. A broader band with a wide base and a low peak would have a lower average density than a sharp band with a narrow base and a high peak. Therefore, both measures taken together provide a better description of the changes in a given band over time.

3.2 Whole Cell Lysate Gel Analysis

At the first time point (0 h) two of the most prominent bands had molecular weights of ~220 kDa and ~50 kDa. These bands most likely contain the myosin heavy chain and actin, respectively. The electrophoretograms consistently had two dense clusters of banding, and one broad, relatively faint region (Fig. 2). Because all twenty-one samples were analyzed using three different gels, a direct comparison of band density could not reliably be made. Therefore, each band's density was expressed as a percent of the total

band density of all the bands studied for measurements of average density, or the entire density of the lane for measurements of trace density.

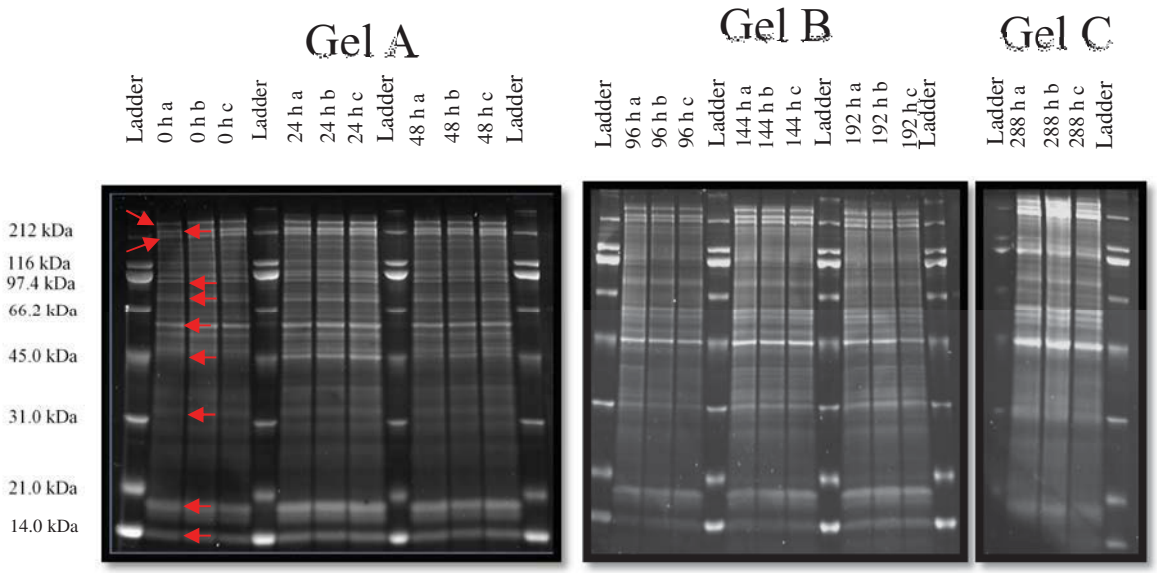

Fig. 2. Electrophoretograms of whole cell lysate (WCL) WCL was extracted from C2C12 myoblasts in 21 cultures over the course of 12 days. Ten bands sampled for densitometry analysis indicated by red lines in the first lane in which they appear.

Band 1 had an average molecular weight of 271.11 kDa and stayed relatively consistent through all time points. When the average density was measured, the band accounted for 11.06% of the total density the ten bands studied at 0 h, dropped slightly to 6.27% after 48 h before dropping to 19.15% 192 h, and again dropping to 11.54% When the total trace density was measured, the band accounted for 4.20% of the lane density, and dropped to 2.05% after 96 h, and eventually returned to 4.38% after 288 h (Fig. 4).

Band 2 had an average molecular weight of 233.24 kDa, and varied only modestly throu34ghout the time course. At 0 h, the band's average density was 11.78% of the 10 bands sampled. Within 24 h, the band dropped to 9.55%, before reaching the greatest

level of 14.16% after 96 h. The relative proportion of the bands average density dropped and rose slightly over the remaining time points eventually reaching 9.14% at the end of the time course. The proportion of the bands density to the total lane density began at 3.71% at 0 h, and increased to 4.09% after 144 h. At the end of the time course, the band's density was 3.01% of the entire lane.

Band 3 had an average molecular weight of 207.58 kDa, and its density increased an appreciable amount during the time course. At 0 h, the band's average density was 11.42% of the 10 bands sampled. Within 48 h, the band dropped to 8.89%, before increasing to 25.16% at the end of the time course. The proportion of the bands density to the total lane density began at 3.96% at 0 h, and increased gradually to 8.02% at the end of the time course.

Band 4 had an average molecular weight of 96.22 kDa, and its density decreased throughout time course before increasing to a value similar to its original value at the beginning of the time course. At 0 h, the band's average density was 9.99% of the 10 bands sampled. After 192 h, the band's density dropped to just 0.47%, before returning to 10.15% at the end of the time course. The proportion of the bands density to the total lane density began at 4.68% at 0 h, and decreased to just 0.10% after 192 h. At the end of the time course, the band's density was 9.12% of the entire lane.

Band 5 had an average molecular weight of 77.22 kDa, and its density was fairly stable through the time course. At 0 h, the band's average density was 6.41% of the 10 bands sampled. After 96 h, the band's density increased to 10.10%, before decreasing to 5.15% at the end of the time course. The proportion of the bands density to the total lane density

began at 2.73% at 0 h, and increased to 6.61% after 96 h. At the end of the time course, the band's density was 5.24% of the entire lane.

Band 6 had an average molecular weight of 56.18 kDa, and its density decreased through the time course before rising slightly at the end. At 0 h, the band's average density was 15.99% of the 10 bands sampled. After 144 h, the band's density had decreased to 4.32%, before increasing to 13.39% at the end of the time course. The proportion of the bands density to the total lane density began at 10.09% at 0 h, and decreased to 2.10% after 96 h. At the end of the time course, the band's density was 3.90% of the entire lane.

Band 7 had an average molecular weight 44.86 kDa, and its density increased dramatically throughout the time course. At 0 h, the band's average density was 2.1% of the 10 bands sampled, and by 144 h, the band's density had increased to 28.06 % before decreasing to 13.39%. The proportion of the bands density to the total lane density began at 0.39% at 0 h, and increased to 4.55% after 24 h. The band decreased to 1.76% at 48 h. At the end of the time course, the band's density was 28.73% of the entire lane, making it one of the most intense bands in any of the sample lanes.

Band 8 had an average molecular weight of 31.29 kDa, and its density remained moderate through the time course. At 0 h, the band's average density was 4.02% of the 10 bands sampled. After 48 h, the band's average density decreased to 3.31%, before increasing to 9.25% at 96 h and then decreasing to 3.78% at the end of the time course. The proportion of the bands density to the total lane density began at 3.88% at 0 h, and decreased to 2.79% after 48 h. The density fluctuated modestly throughout the remainder of the time course, becoming 4.64% of the entire lane at the end of the time course.

Band 9 had an average molecular weight of 18.39 kDa, and is defined as a very broad, albeit faint band, that seems to separate into two or three smaller bands during the time course. At 0 h, the band's average density was 14.88% of the 10 bands sampled. Within 48 h, the band's average density had increased to 22.28%, before decreasing to 7.68% after 144 h, increasing again to 12.59% at 192 h and dropping to 6.56% by the end of the time course. The proportion of the bands density to the total lane density began at 25.67% at 0 h, and increased to 33.04% after 48 h, and decreasing to 19.45% after 144 and increasing to 25.10% after 192 and decreasing to 13.51% by the end of the time course.

Band 10 had an average molecular weight of 14.04 kDa, and is also defined as a very broad band that seems to separate into multiple bands through the time course. At 0 h, the band's average density was 12.25% of the 10 bands sampled. Within 48 h, the band's average density had increased to 14.50%, before decreasing to 3.56% after 144 h, increasing again to 5.12% at 192 h and dropping again to 1.18% by the end of the time course. The proportion of the bands density to the total lane density began at 12.60% at 0 h, and increased to 14.57% after 48 h, and decreasing to 2.61% after 144 and again increased to 6.65% after 192 h and decreasing to just 0.63% by the end of the time course.

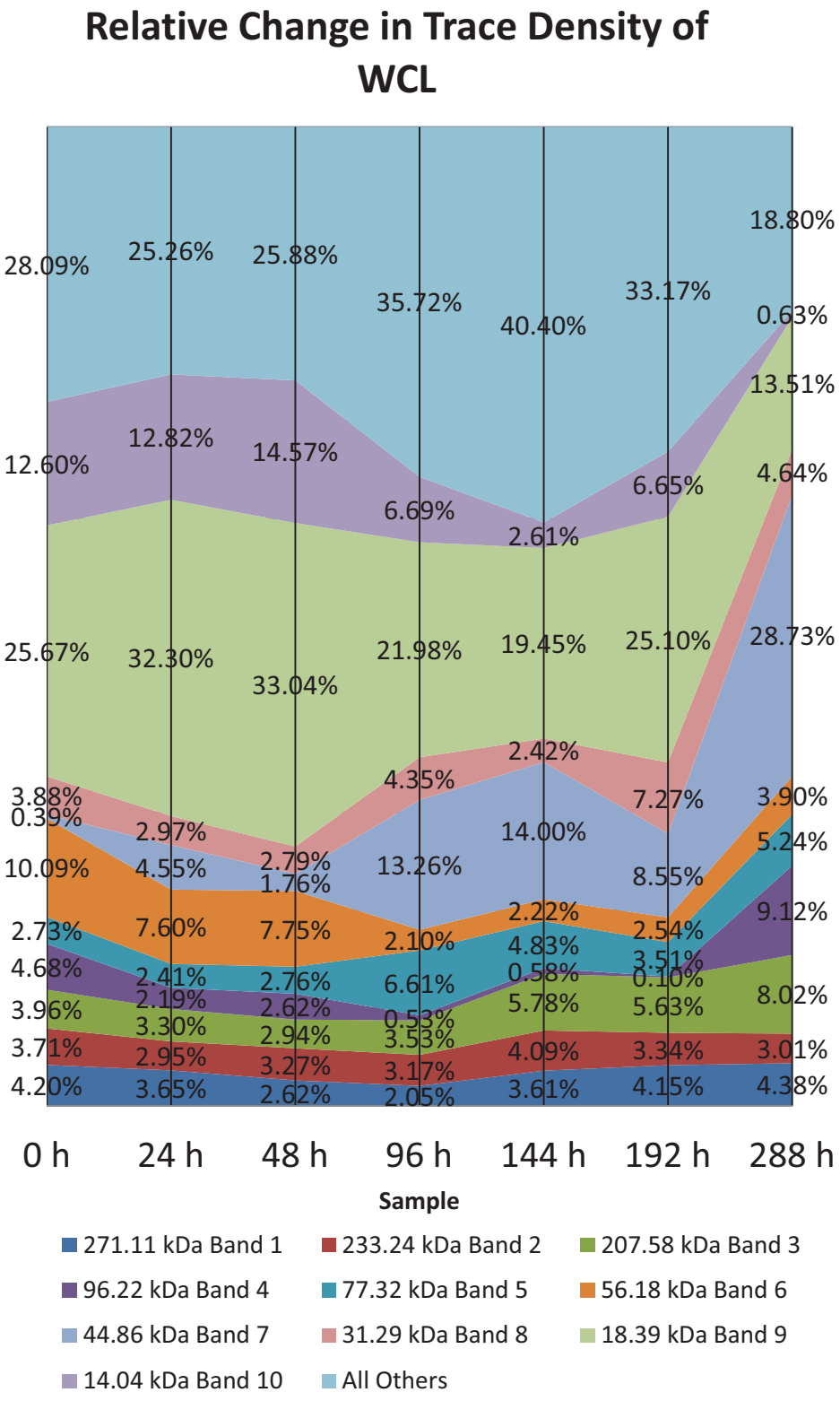

Fig. 3. Relative Change in Trace Density of WCL. Area chart showing changes in trace density of selected bands expressed as a percentage of the sum density of all bands in the lane occupied by a given time point sample.

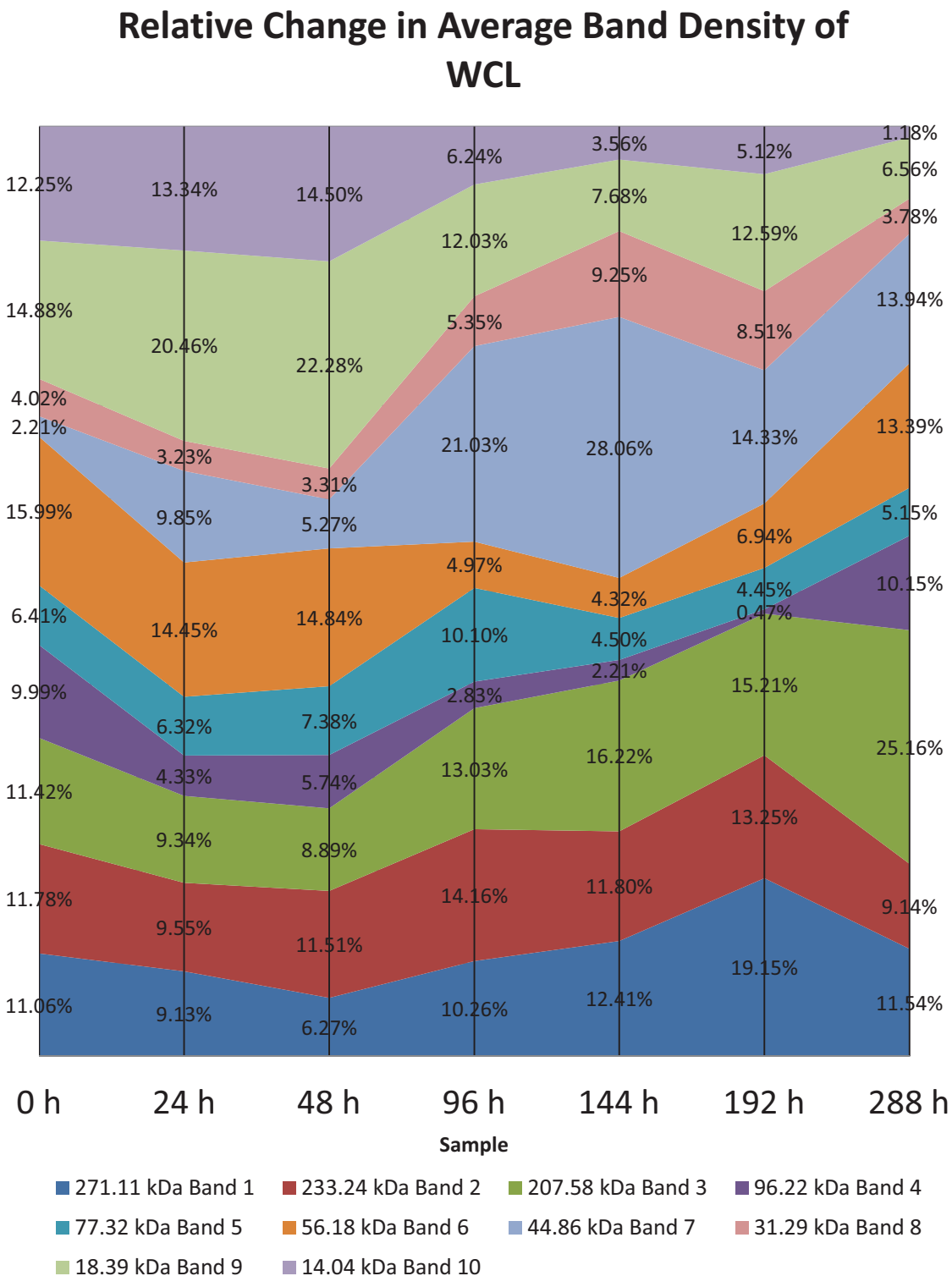

Fig. 4. Relative Change in Average Band Density of WCL. Area chart showing changes in average density of selected bands expressed as a percentage of the sum density of all twelve bands sampled for analysis.

3.3 Detergent Insoluble Portion Gel Analysis

The second time course yielded two sets of samples, the detergent-insoluble portion (DSP), and the detergent insoluble portion (DIP). Twelve of the most apparent bands were selected from electrophoretogram containing the DIP. By matching peaks in side-by-side comparisons of densitometry plots in individual lanes, it can be determined what proteins are enriched in either sample.

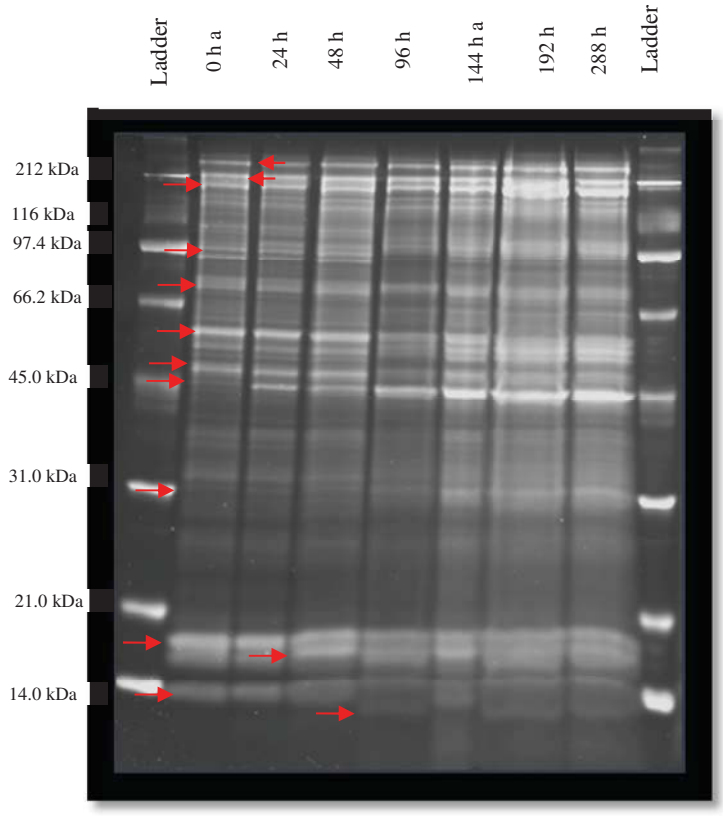

Fig. 5. Electrophoretogram of Detergent Insolubule Portion (DIP) WCL was extracted from C2C12 myoblasts in 7 cultures over the course of 12 days. Twelve bands sampled for densitometry analysis indicated by red lines in the first lane in which they appear.

The first band measured in the DIP electrophoretogram had an average molecular weight of 252.09 kDa. and remained fairly consistent through the time course. The band had an average density 11.35 of the twelve bands sampled at 0 h. It reached its peak average

density, which was 15.68% of the twelve bands sampled, after 96 h. The density receded to 12.18% at the end of the time course. The trace density gradually increased from being 3.15% of the twelve bands sampled to 8.39%.

Band 2 in the DIP had an average molecular weight of 214.09 kDa and remained somewhat consistent through the time course also. At 0 h, the band had an average molecular weight of 11.24%, and declined after 24 h to 7.52%, and later to 4.95%, after 192 h. It reached its highest amount, 18.21%, after 288 h, at the end of the time course. The trace density changed over time in the same way, declining from the initial value of 2.77% until beginning to rise again after 24 h and again falling off again after 96 h, being 5.11% at the end of the time course.

Band 3 in the DIP had an average molecular weight of 188 kDa and became broader as the time course progressed. Its average density at 0 h was 6.21% and exhibited a somewhat steady decline, becoming just 0.69% at the end of the time course. The trace density, however shows a very steady increase, from 2.28% at 0 h to 9.64 kDa after 288 h

Band 4 in the DIP had an average molecular weight of 88.92 kDa and became sharper as the time course progressed. Its average density increased until 96 h when it was 17.04% of the twelve bands sampled. The average density decreased before rising to its peak, which was 17.25% at 192 h. At the end of the time course, the average density was 2.55% of the twelve bands sampled. The trace density increases slightly from 1.93% at 0 h until reaching 2.37% after 48 h, decreasing to just 0.02% at 96 h, and remaining less than 1% through the remainder of the time course.

Band 5 in the DIP had an average molecular weight of 74.44 kDa and its density fluctuated through the time course. Its average density at 0 h was 18.39% of the twelve bands sampled and dropped significantly after 96 h, to 6.97%, rising to 9.35% after 144 h. At 192 h, the average density was measured to be just 1.09% of the twelve bands sampled. The average density of band 5 at the end of the time course was 9.60%. The trace density of band 5 was 5.88% of the total density of the lane at 0 h, but decreased after 24 h, and rose to 9.79% at 48 h. The band's density decreased 4.35% after 96 h, and rose again to 6.92% of the entire lane at 144 h, before decreasing to just 0.51% at the end of the time course.

Band 6 in the DIP had an average molecular weight of 57.78 kDa, and became sharper through the time course. Its average density began fairly low; being 1.12% of the twelve bands sampled, but became 20.06% after 192 h. At the end of the time course, band 6's average density was 19.82% of the twelve bands sampled. The trace density of band 6 was 8.71% of the entire lane, and increased to 11.16% after 48 h. After 96 h, its trace density dropped to 5.66% and dropped again to 0.24% at 192 h. At the end of the time course, the trace density of band 6 was 8.94% of the entire lane.

Band 7 in the DIP had an average molecular weight of 45.20 kDa, and became dramatically more dense as the time course progressed. Its average density at 0 h was 1.03% of the twelve bands sampled but increased to 10.43% at the end of the time course. The trace density of band 7 was just 0.27% of the entire lane, but was 28.23% of the lane's density at the end of the time course.

Band 8 in the DIP had an average molecular weight of 31.18 kDa, and became gradually more broad through the time course. At 0 h, band 8's average density was 1.03% of the twelve bands sampled. After 96 h, it rose to 9.12%, and increased further to 10.43% at the end of the time course. The trace density was just 0.15% of the entire lane at 0 h, and gradually increased to 9.60% of the entire lane at the end of the time course.

Band 9 separated into two distinct bands over the time course. The band with the higher average molecular weight, 17.73 was designated as band 9 through the entire time course. Band 9's average density was 16.64% of the twelve bands sampled at 0 h, and 30.93% after 24 h. After 48 h a new band had emerged from it, and it was thereafter considered to be band 10. The average density of band 9 decreased to being 9.80% of the 12 bands samples as a result. The band's average density had decreased to 4.13% at the end of the time course. The band's trace density began at 38.95% at the beginning of the time course, and decreased to 3.02% at the end of the time course.

Band 10 emerged from band 9 after 48 h, when it could be recognized as an independent peak with an average molecular weight of 16.77 kDa. Its average density 48 h after the time course had begun was 7.18% of the twelve bands sampled. Its average density remained fairly consistent through the time course, being 4.13% of the twelve bands sampled at the end of the time course. Its trace density 48 h after the time course had begun was 6.80% of the entire lane and was 5.40% of the entire lane at the end of the time course.

Band 11 also separated into two distinct bands over the time course. After 96 h, there were two distinct peaks. The band with the higher average molecular weight, 13.65 was

designated as band 11 through the entire time course whereas the band with the lower average molecular weight was considered to be band 12. Band 11 began at 0 h with a density that was 9.02% of the twelve bands sampled, and after 96 h, when band 12 emerged from it, the density became 2.96% of the twelve bands sampled. At the end of the time course, the band's density was 2.28% of the twelve bands sampled

Band 12 emerged from band 11 after 96 h, when it could be recognized as an independent peak with an average molecular weight of 13.29 kDa. Its average density 96 h after the time course had begun was 1.16% of the twelve bands sampled. Its average density remained fairly consistent through the time course, being 1.72% of the twelve bands sampled at the end of the time course. Its trace density 96 h after the time course had begun was 1.42% of the twelve bands sampled, and was 1.29% at the end of the time course.

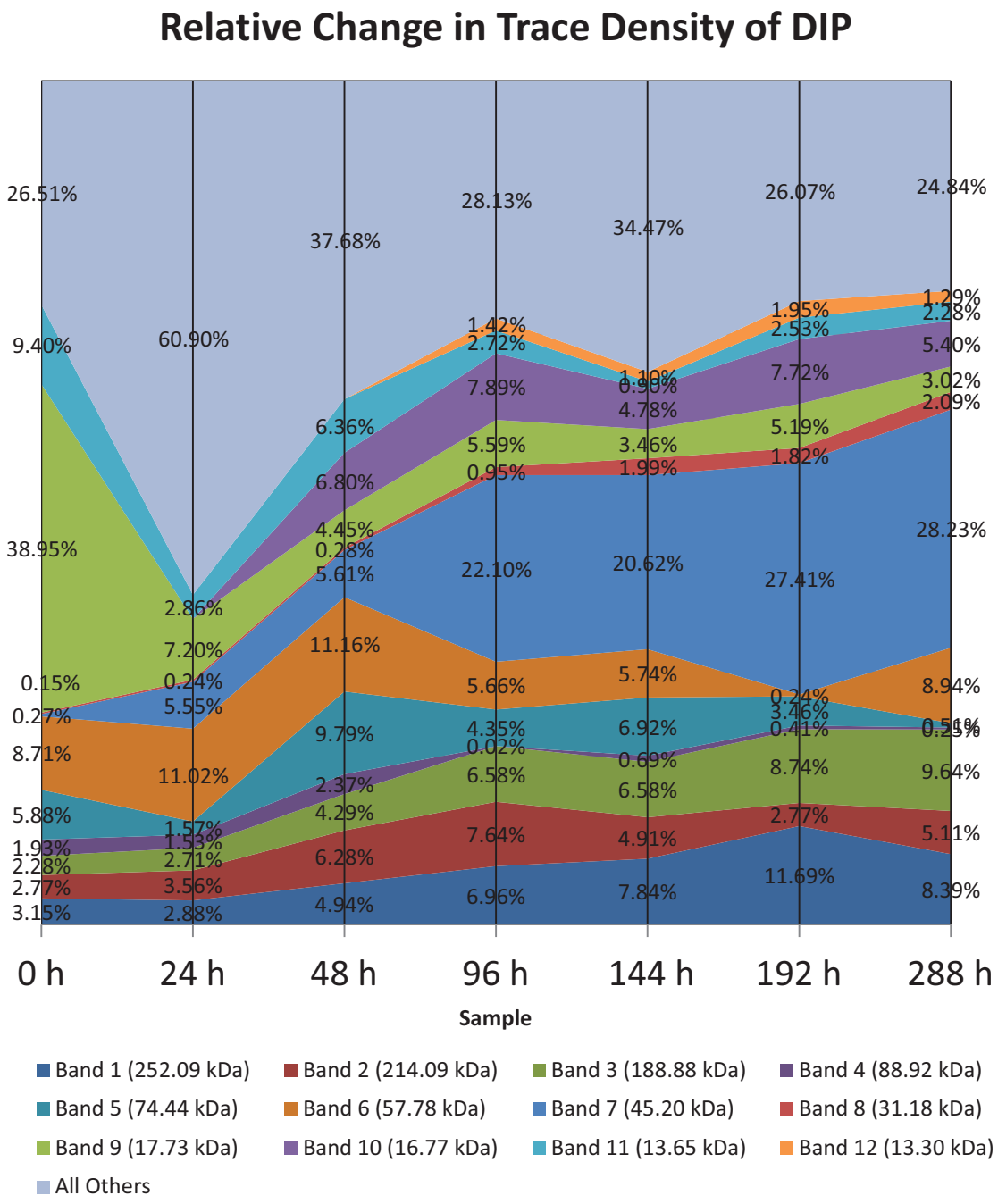

Fig. 6. Relative Change in Trace Density of DIP. Area chart showing changes in trace density of selected bands expressed as a percentage of the sum density of all bands in the lane occupied by a given time point sample.

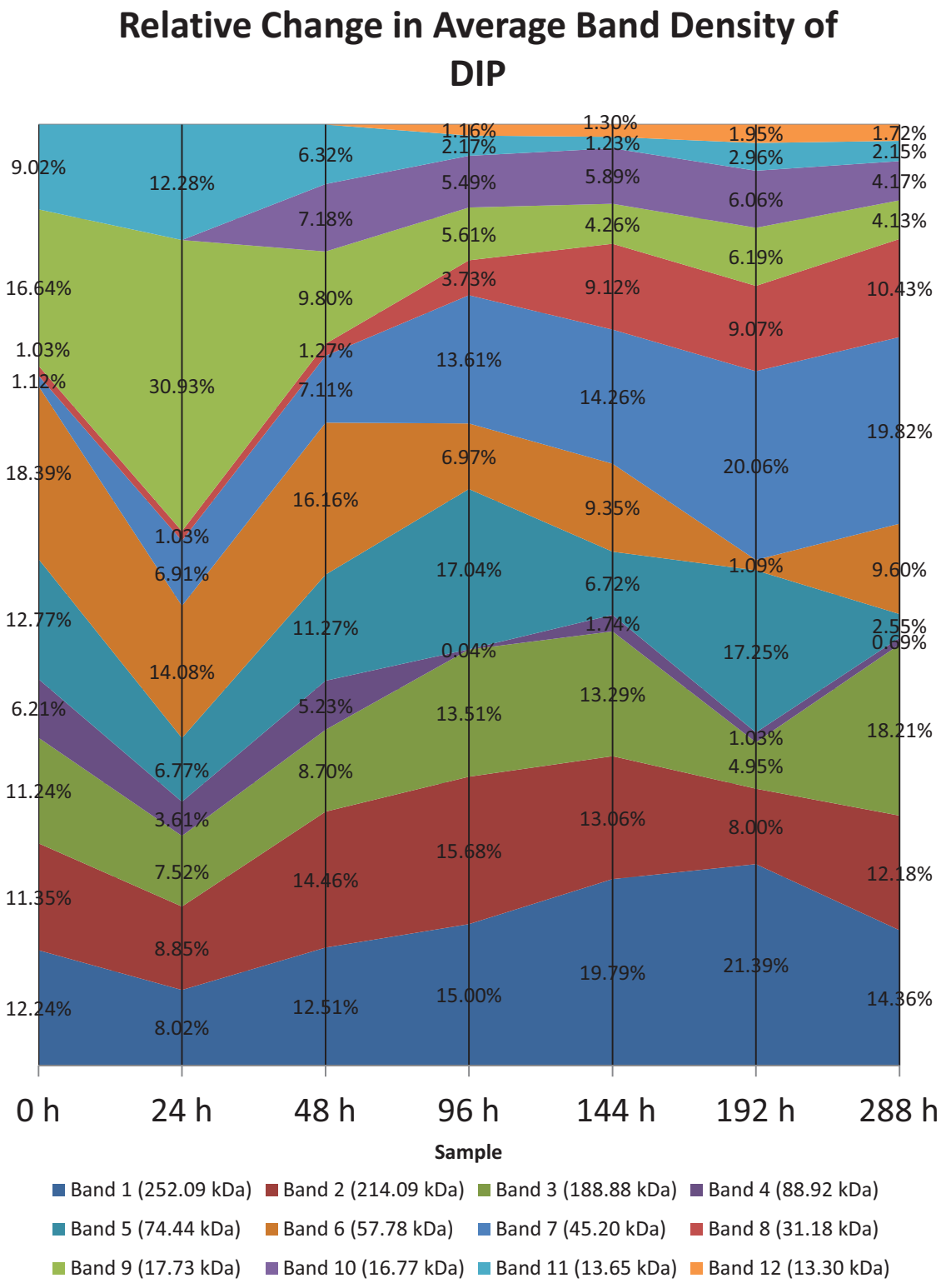

Fig. 7. Relative Change in Trace Density of DIP Area chart showing changes in average density of selected bands expressed as a percentage of the sum density of all twelve bands sampled for analysis.

3.4 Detergent Soluble Portion Gel Analysis

Eleven bands from the electrophoretogram containing the DSP that appeared to appear across every time point were selected to compare densitometry across different time points.

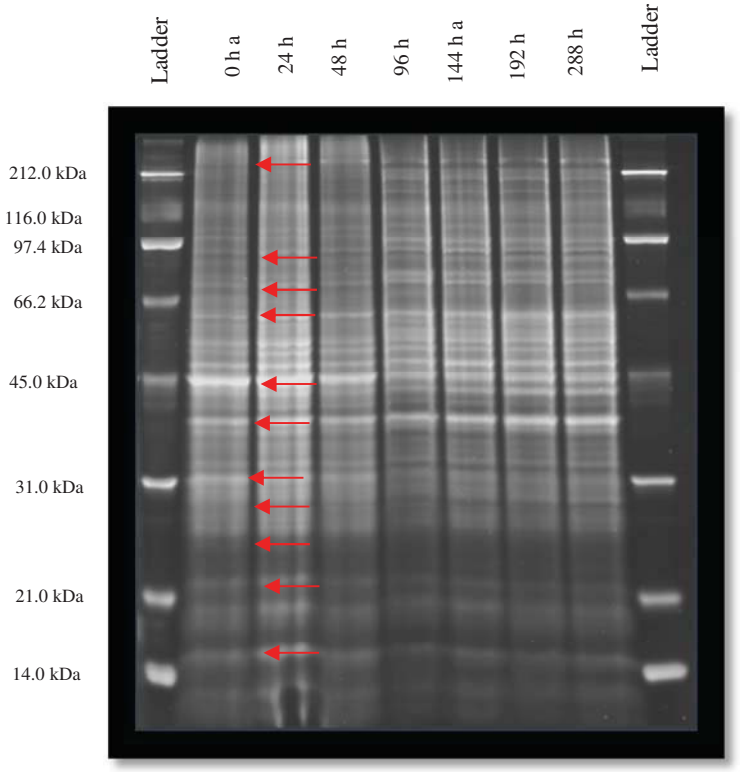

Fig. 8. Electrophoretogram of Detergent Solubule Portion (DSP) WCL was extracted from C2C12 myoblasts in 7 cultures over the course of 12 days. Eleven bands sampled for densitometry analysis indicated by red lines in the first lane in which they appear.

The first band measured in the DSP electrophoretogram had an average molecular weight of 286.72 kDa, and its density remained fairly consistent through the time course. The band had an average density 7.16% of the eleven bands sampled at 0 h. Its average density at the end of the time course was 7.04% of the eleven bands sampled. The trace density of the band was 3.17% of the entire lane at 0 h, and 3.10% at the end of the time course.

Band 2 in the DSP had an average molecular weight of 91.96 kDa, and changed little through the time course. The band had an average density 6.00% of the eleven bands sampled at 0 h, after 96 h, the band's density had decreased to 1.78% of the eleven bands sampled. The average density of the band thereafter began to increase until then end of the time course when it was 8.05% of the bands sampled. The trace density changed from being 0.97% of the entire lane at 0 h, to 3.13% of the entire lane at the end of time course, gradually increasing from 192 h onward.

Band 3 in the DSP had an average molecular weight of 72.83 kDa, and also changed little through the time course. The band initially had an average density of 4.50% at 0 h and its average density increased until 48 h, when its average density was 7.36% of the eleven bands measured. Its average density had decreased to 0.83% of the twelve bands sampled by 192 h, but increased to 9.56% after 288 h. The trace density increased from 0.73% of the entire lane to 1.85% of the entire lane after 288 h.

Band 4 in the DSP had an average molecular weight of 60.97 kDa. The average density of the band at 0 h was 5.16% of the eleven bands sampled but increased to 10.80% after 48 h. Its average density increased to the peak value of 13.28% after 192 h. Its average density decreased to 9.56% of the eleven at the conclusion of the time course. The trace density increased from 2.82% at 0 h to 9.84% after 192 h. At the end of the time course the trace density of band 4 was 6.31% of the entire lane.

Band 5 in the DSP had an average molecular weight of 44.23 kDa, and decreased significantly through the time course. Its average density at beginning of the time course constituted 28.80% of that of the eleven bands sampled. Its average density decreased

until the end of the time course until its average was 13.62% of the eleven bands sampled. The trace density decreased from being 27.24% of the entire lane at the beginning of the time course to 8.10% at the end.

Band 6 in the DSP had an average molecular weight of 38.49 kDa, and became much sharper and generally denser as the time course progressed. Its average density was 15.84% of the eleven bands sampled at 0 h, and increased to 38.13% after 96 h. At the end of the time course, the average density was 29.45% of the eleven bands sampled. At 0 h, the trace density was 6.56% of entire lane, and after 192 h the trace density was 26.18% of the entire lane. At the conclusion of the time course, the trace density was 15.24% of the entire lane

Band 7 in the DSP had an average molecular weight of 31.49 kDa. Its average density was 12.83% of the eleven bands sampled at 0 h, and decreased to 7.07% by the end of the time course. The trace density of band remained fairly consistent, changing from 6.26% of the entire lane at 0 h, to 4.76% at 288 h.

Band 8 in the DSP had an average molecular weight of 22.15 kDa. Its average density changed little through the time course, being 3.71% of the eleven bands sampled at 0 h, and 2.27% after 288 h. At 0 h, the trace density was 3.07% of entire lane, and after 288 h the trace density was 1.18% of the entire lane

Band 9 in the DSP had an average molecular weight of 19.38 kDa. Its average density remained consistent through the time course, being 5.74% of the eleven bands sampled at 0 h, and 5.88% after 288 h. The trace density of band remained fairly consistent, changing from 6.70% of the entire lane at 0 h, to 8.13% at 288 h.

Band 10 in the DSP had an average molecular weight of 15.44 kDa. Its average density at 0 h was 5.87% of the eleven bands sampled, but increased to 11.22% after 24 h. The decreased to 4.19% of the eleven bands sampled after 96 h, and remained fairly consistent through the remainder of the time course, being 5.16% of the eleven bands sampled after 288 h. At 0 h, the trace density was 6.59% of entire lane, and after 288 h the trace density was 5.48% of the entire lane.

Band 11 in the DSP had an average molecular weight of 12.61 kDa. Its average density at 0 h was 3.91% of the eleven bands sampled, and decreased to just 0.26% of the eleven bands sampled after 192 h, being otherwise fairly consistent through the time course. The trace density increased from being 5.43% of the entire lane at the beginning of the time course to 7.25% at the end. The trace density had decreased to just 0.03% of the entire lane by 192 h, and was 3.34% of the entire lane by the end of the time course.

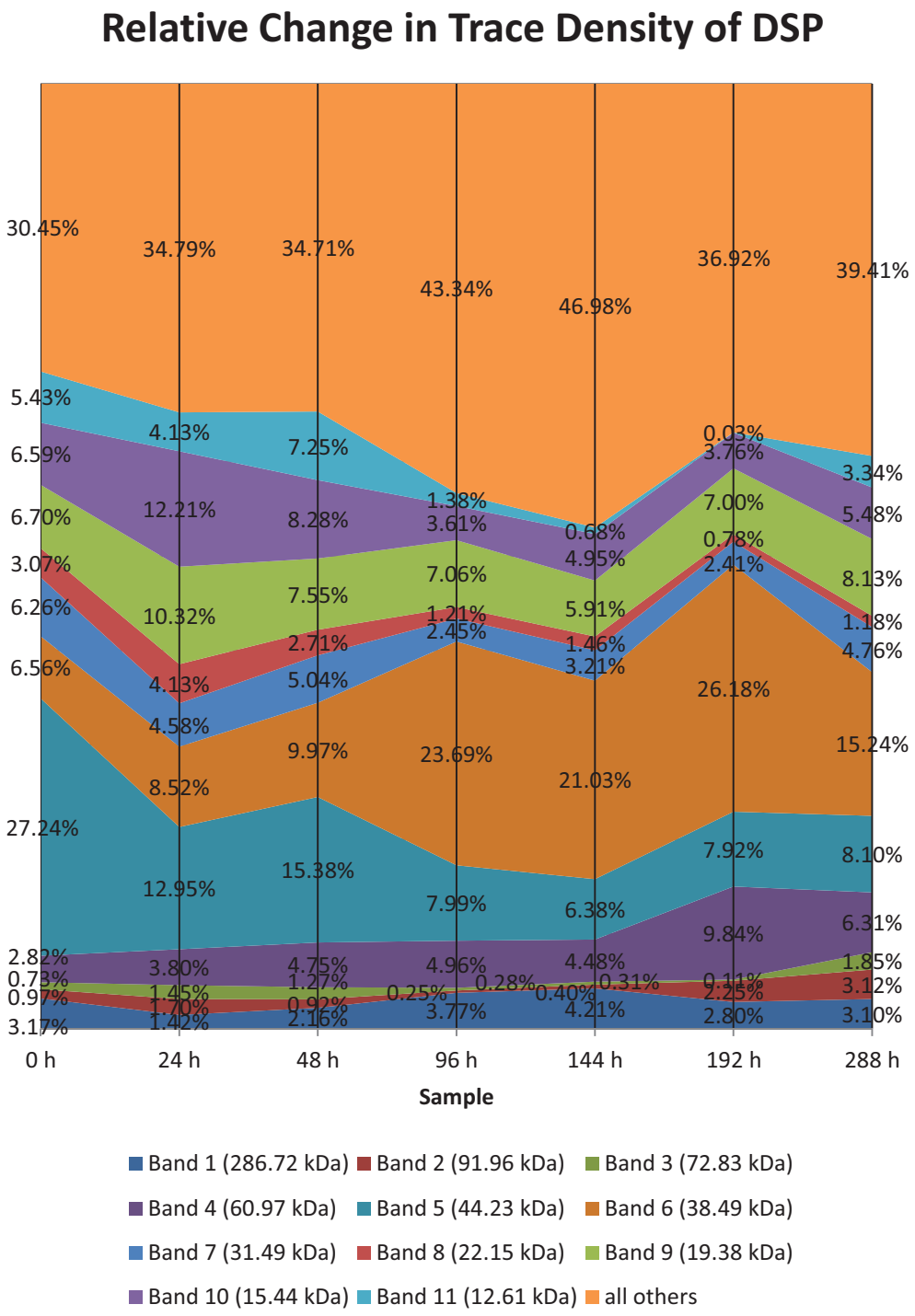

Fig. 9. Relative Change in Trace Density of DSP Area chart showing changes in trace density of selected bands expressed as a percentage of the sum density of all bands in the lane occupied by a given time point sample.

Fig. 10. Relative Change in Average Density of DSP Area chart showing changes in average density of selected bands expressed as a percentage of the sum density of all eleven bands sampled for analysis.

3.5 LC-MS-MS Analysis

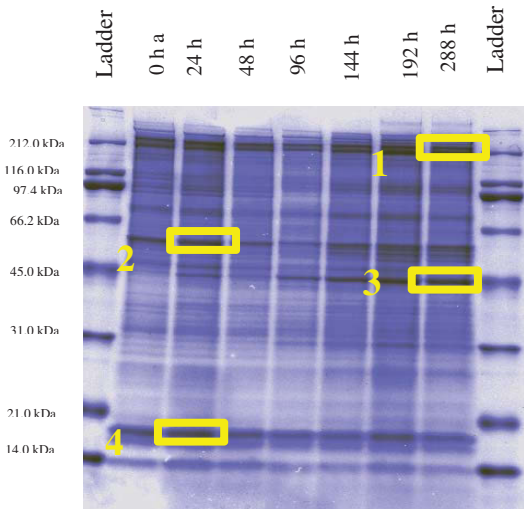

Fig. 1. Electrophoretogram of the detergent insoluble portion (DIP). Bands excised for LS-MS-MS analysis are indicated by numbered yellow boxes

Protein bands indicated in figure 1 were excised and submitted to The Ohio State University Mass Spectrometry and Proteomics Facility for Capillary-liquid chromatogragraphy-nanospray tandem Mass Spectroscopy LC-MS-MS.

The results indicated that bands 2 and 3 in the 288 h DIP (LS-MS-MS Sample 1) were dominated by four different forms of myosin, mainly myosin-1, myosin-9 and myosin-8 (Table 1). 6.11% of the bands content was shown to be the ferritin light chain. 4.17% of the bands' content was shown to be plectin. Two other proteins, nestin and fibronectin, accounted for 2.62% and 2.44% of the bands' content, respectively. Filamin-a was shown to constitute 1.75% of the two bands. All other proteins accounted for less than 1% of the bands content.

LS-MS-MS Sample 1 (288 h DIP Bands 2 and 3) Results						
Description	**Nominal MW (kDa)**	**Experimental average MW (kDa)**	**Relative Proportion**	**Score**	**Percent Coverage**	**Accession**
Myosin-1	224.116		36.47%	1762	40	MYH1_MOUSE
Myosin-9	227.429		17.63%	1267	28	MYH9_MOUSE
Myosin-8	223.653		17.45%	1111	24	MYH8_MOUSE
Myosin-7	223.539		8.38%	478		MYH7_MOUSE
Plectin	535.828		4.71%	689	5	PLEC_MOUSE
Filamin-A	283.897		1.75%	166	5	FLNA_MOUSE
Filamin-B	280.103		0.70%	122	2	FLNB_MOUSE
Nestin	207.627		2.62%	287	6	NEST_MOUSE
Fibronectin	276.017		2.44%	229	6	FINC_MOUSE
Nascent polypeptide-associated complex subunit alpha, muscle-specific form	221.277		0.70%	125	2	NACAM_MOUSE
Talin-1	271.82		0.35%	80	1	TLN1_MOUSE
Ferritin light chain 1	20.847		6.11%	68	8	FRIL1_MOUSE
Cytoplasmic dynein	534.447		0.17%	60	0	DYHC1_MOUSE
Xin actin-binding repeat-containing protein	124.096		0.52%	53	0	XIRP1_MOUSE

Table 1. LS-MS-MS Sample 1 (288 h DIP Bands 2 and 3) Results. LS-MS-MS Sample 1 corresponds with the 288 h DIP Bands 2 and 3 as identified in the densitometry analysis. The bands had average molecular weights of 214.09 kDa and 188.88 kDa, respectively. The highest scores for a *Mus musculus* protein were assessed to different isoforms of myosin, which also had the highest relative proportion within the band.

Band 4 from the 24 h DIP (LS-MS-MS Sample 2)was shown to be mainly (84.55%) vimentin. There were minor amounts of alpha enolase (5.35%), desmin (3.07%) and pyruvate kinase isozymes M1 and M2 (1.53%). There was also a small amount of a 60 kDa heat shock protein. All others were less than 1% of the band's content.

LS-MS-MS Sample 2 (24 h DIP Band 6) Results					
Description	**MW (kDa)**	**Relative Proportion of identified peptides**	**Score**	**Percent Coverage**	**Accession**
Vimentin	53.712	84.55%	2763	71	VIME_MOUSE
Desmin	53.522	3.07%	445	37	DESM_MOUSE
Alpha-enolase	47.453	5.35%	799	62	ENOA_MOUSE
60 kDa heat shock protein	61.088	1.44%	401	34	CH60_MOUSE
Pyruvate kinase isozymes M1/M2	58.378	1.53%	320	32	KPYM_MOUSE
Protein disulfide-isomerase	48.469	0.92%	214	26	PDIA6_MOUSE
ATP synthase subunit alpha, mitochondrial	59.83	0.32%	174	9	ATPA_MOUSE
Adenylyl cyclase-associated protein 1	51.875	0.37%	138	8	CAP1_MOUSE
T-complex protein 1 subunit beta	57.783	0.43%	116	13	TCPB_MOUSE
Aspartate--tRNA ligase	57.567	0.75%	112	18	SYDC_MOUSE
Protein disulfide-isomerase	57.099	0.43%	93	6	PDIA3_MOUSE
Drebrin-like protein	48.955	0.09%	86	3	DBNL_MOUSE
Polymerase I and transcript release factor	43.927	0.21%	81	7	PTRF_MOUSE
Glucose-6-phosphate isomerase	62.955	0.15%	78	3	G6PI_MOUSE
Polypyrimidine tract-binding protein 1	56.671	0.08%	78	5	PTBP1_MOUSE
Nucleosome assembly protein 1-like 1	45.602	0.20%	60	7	NP1L1_MOUSE
Nucleosome assembly protein 1-like 4	42.824	0.11%	59	4	NP1L4_MOUSE

Table 2. LS-MS-MS Sample 2 (24 h DIP Band6) Results. LS-MS-MS Sample 2 corresponds with the 24 h DIP Band 6 as identified in the densitometry analysis. The band had an average molecular weight of 57.78 kDa. The highest score for a *Mus musculus* protein was assessed to vimentin, which also had the highest relative proportion within the band.

Band 7 from the 288 h DIP (LS-MS-MS Sample 3) was shown to be fairly diverse (Table 2, with a majority (22.65%) being a mitochondrial cytochrome b-1complex, and 12.53% belonging to vimentin, the dominant protein in DIP Band 4. Fructose biphosphate aldolase, serpin H1, and the 60s ribosomal protein L1 all were 9.88% of the band's content. Mitochondrial citrate synthase was 6.75% and 3-ketoacyl-CoA thyolase was 3.86%, and an NADH dehydrogenase was 3.13% of the band. There were various other

proteins within this band, none of which constituted greater than 3% of the band's content.

LS-MS-MS Sample 3 (288 h DIP Band 7) Results					
Description	**Nominal MW (kDa)**	**Relative Proportion of identified peptides**	**Score**	**Percent Coverage**	**Accession**
Cytochrome b-c1 complex subunit 2, mitochondrial	48.262	22.65%	335	24	QCR2_MOUSE
Vimentin	53.712	12.53%	199	13	VIME_MOUSE
Fructose-bisphosphate aldolase A	39.787	9.88%	187	19	ALDOA_MOUSE
Serpin H1	46.618	9.88%	190	18	SERPH_MOUSE
60S ribosomal protein L3	46.366	9.88%	169	18	RL3_MOUSE
Citrate synthase, mitochondrial	51.988	6.75%	103	10	CISY_MOUSE
3-ketoacyl-CoA thiolase, mitochondrial	42.26	3.86%	100	4	THIM_MOUSE
NADH dehydrogenase [ubiquinone] iron-sulfur protein 2, mitochondrial	52.991	3.13%	48	4	NDUS2_MOUSE
Leukocyte surface antigen CD47	33.589	2.41%	36	4	CD47_MOUSE
Junctional sarcoplasmic reticulum protein 1	36.242	2.17%	74	4	JSPR1_MOUSE
Troponin T, cardiac muscle	35.804	2.17%	50	4	TNNT2_MOUSE
Beta-centractin	42.369	1.93%	93	4	ACTY_MOUSE
Protein NDRG1	43.437	1.93%	72	3	NDRG1_MOUSE
Alpha-2-macroglobulin receptor-associated protein	42.189	1.93%	53	3	AMRP_MOUSE
Macrophage-capping protein	39.501	1.93%	42	7	CAPG_MOUSE
28S ribosomal protein S27, mitochondrial	48.147	1.69%	58	2	RT27_MOUSE
Transducin beta-like protein 2	50.179	1.69%	57	2	TBL2_MOUSE
Medium-chain specific acyl-CoA dehydrogenase, mitochondrial	46.908	1.69%	41	2	ACADM_MOUSE

Table 3. LS-MS-MS Sample 2 (288 h DIP Band 7 Results. LS-MS-MS Sample 3 corresponds with the 288 h DIP Band 7 as identified in the densitometry analysis. The band had an average molecular weight of 45.20**.** The highest score for a *Mus musculus* protein was assessed to subnunit 2 of a mitochondrial cytochrome b-c1 complex, which also had the highest relative proportion within the band.

About half (56.91% of the content of band 12 from the 24 h DIP (LS-MS-MS Sample 4) was shown to be a peptidyl prolyl cis/trans isomerase A, whereas 20.88% was a putative RNA binding protein (Table 4). Nucleoside diphosphate kinase A and B were 7.27% and 10.54% of the band, respectively. A nucleotide binding protein constituted 2.56% of the content of the band. The remaining protein to contribute significantly to the band's content was the ferritin light chain 1.

LS-MS-MS Sample 4 (24 h DIP Band 11) Results					
Description	**MW (kDa)**	**Relative Proportion of identified peptides**	**Score**	**Percent Coverage**	**Accession**
Putative RNA-binding protein 3	16.595	20.88%	212	47	RBM3_MOUSE
Peptidyl-prolyl cis-trans isomerase A	18.131	56.91%	202	55	PPIA_MOUSE
Nucleoside diphosphate kinase B	17.466	10.54%	102	33	NDKB_MOUSE
Nucleoside diphosphate kinase A	17.311	7.27%	88	21	NDKA_MOUSE
Ferritin light chain 1	20.847	1.64%	79	8	FRIL1_MOUSE
Histidine triad nucleotide-binding protein 1	13.882	2.56%	28	11	HINT1_MOUSE
Uncharacterized protein C2orf71 homolog	140.808	0.20%	25	0	CB071_MOUSE

Table 4. LS-MS-MS Sample 2 (24 h DIP Band 11) Results. LS-MS-MS Sample 4 corresponds with the 24 h DIP Band 11 as identified in the densitometry analysis. The band had an average molecular weight of 13.65 kDa. The highest score for a *Mus musculus* protein was assessed to a peptidyl-prolyl cis-trans isomerase A, which also had the highest relative proportion within the band.

4. Discussion

4.1 Introduction

Whole cell lysates were acquired from C2C12 myoblast cultures that were allowed to differentiate for a specified period of time. Ten bands were selected by their prominence, which therefore made them easy to identify in all sample lanes in spite of the complexity of the protein profile. Since the gels used had only 18 sample lanes, In order to run each triplicate sample concurrently with molecular weight and quantity standards, the samples had to be run on three separate gels. This was done to obtain an average value based on the densitometry measurements, Although the gels were run at the same time under the same conditions, there were apparent variations between gels that prevented a side-by-side comparison of densitometry. Instead, bands were compared as percentages of the sum density of the lane or the bands sampled. Later, another time course yielded two separate samples, a detergent soluble portion, and a detergent insoluble sample. Due to the reduced complexity of the sample profile, various trends were detected in the bands sampled. Finally, samples from each of the seven time points in each of the sample were compared to each other on the same gel and from these comparisons, it can inferred which protein bands are enriched in a particular sample at a particular time.

4.2 Band Trends

There are three high molecular weight bands (average weights of 271.11 kDa, 233.24 kDa, and 207.58 kDa, respectively, in the WCL; identified as band 1, band 2 and band 3

in either the WCL or DIP) that remain almost unchanged through the entirety of the time course. Among these three, one of these seems to be apparent in both the DIP and the DSP (Identified as Band 1 in both the DIP and the DSP).

There is a mid-molecular weight protein (average molecular weight of 56.18 kDa in the WCL; identified as band 6 in the WCL), that is one of the boldest bands in the lane occupied by the 0 h sample, but gradually becomes eclipsed by other bands, to the point where it cannot easily be distinguished from adjacent bands in the lane without examining the lane's densitometry profile.

Perhaps the most interesting change occurs in the band identified as band 7 in the WCL, with an average molecular weight of 44.86 kDa in the WCL, is virtually undetectable in the 0 h sample (only 0.39% of entire lane's trace density in the WCL, 0.27% in the DIP). The band is by far the boldest band in the 288 h sample (28.73% of entire lane's trace density in the WCL, 28.23% in the DIP), and for this reason, the initial observations confused it with band 6 in the 2^{nd} and 3^{rd} gel, which is the brightest band in the 0 h sample. Moreover, there is a band with an average molecular weight of 45.20 kDa in the DSP (identified as band 5) that is initially the boldest (27.04% of the entire lane's trace density in the 0 h sample) and is reduced to 8.10% of the entire lanes trace density in the 288 h sample.

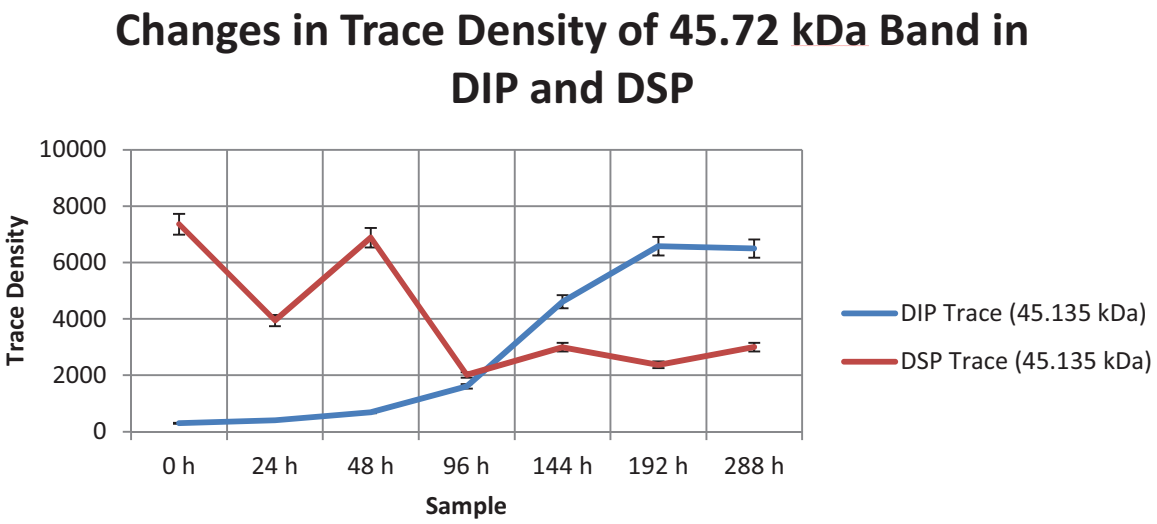

Fig. 11. Changes in Trace Density of 45.72 kDa Band in DIP and DSP. Line graph showing relative changes in the density traces of a band with an average molecular weight of 45.72 kDa in the DIP and DSP

There were two very broad, low molecular weight bands in the WCL (identified as band 9 and band 10; average molecular weights of 18.39 kDa and 14.04 kDa, respectively). The bands are enriched in the DIP (identified as bands 9 and 11 in the DIP), and since there were fewer proteins in the DIP to obscure these bands, it was first observed that these two bands separate into four or more bands through the time course. This implies that prior to cellular differentiation, there is a host of proteins of very similar molecular weight, but through the course of differentiation the molecular weights of these proteins either increase or decrease due to post translational modifications, such as DNA binding to small transcription factors, or the accumulation or dispersal of cofactors to or from other varieties of low molecular weight proteins such as kinases. Alternatively, these changes could be product of differential expression. Indeed, low molecular weight

proteins such as transcription factors vary in expression levels through the entirety of the differentiation.

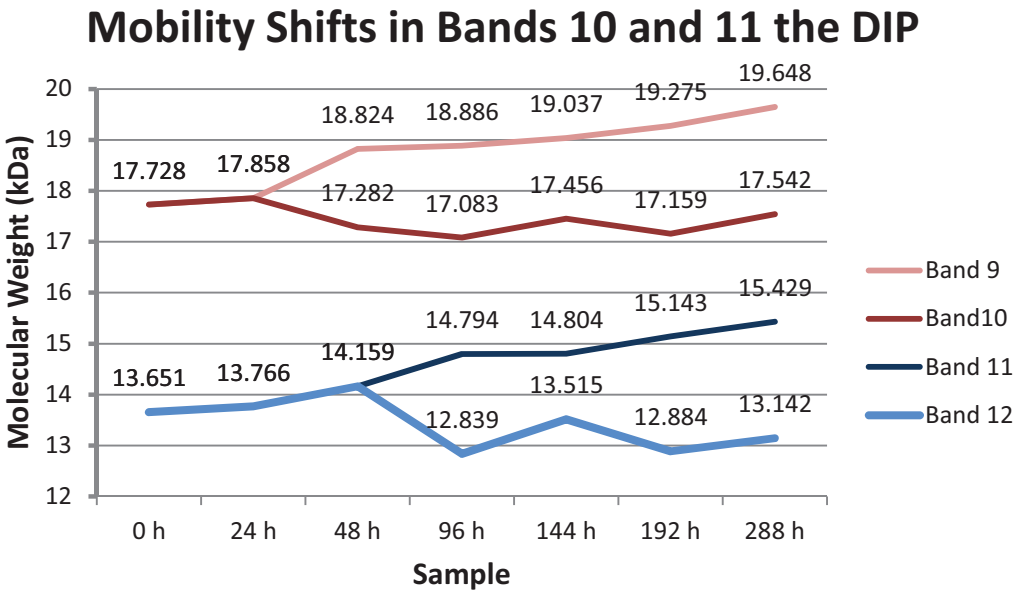

Fig. 12. a: Mobility Shifts in Bands 10 and 11 Line graph showing the changes in the molecular weights of low molecular weight proteins that result in division of band 9 and band 11, resulting in the emergence of band 10 and band 11 in the DIP.

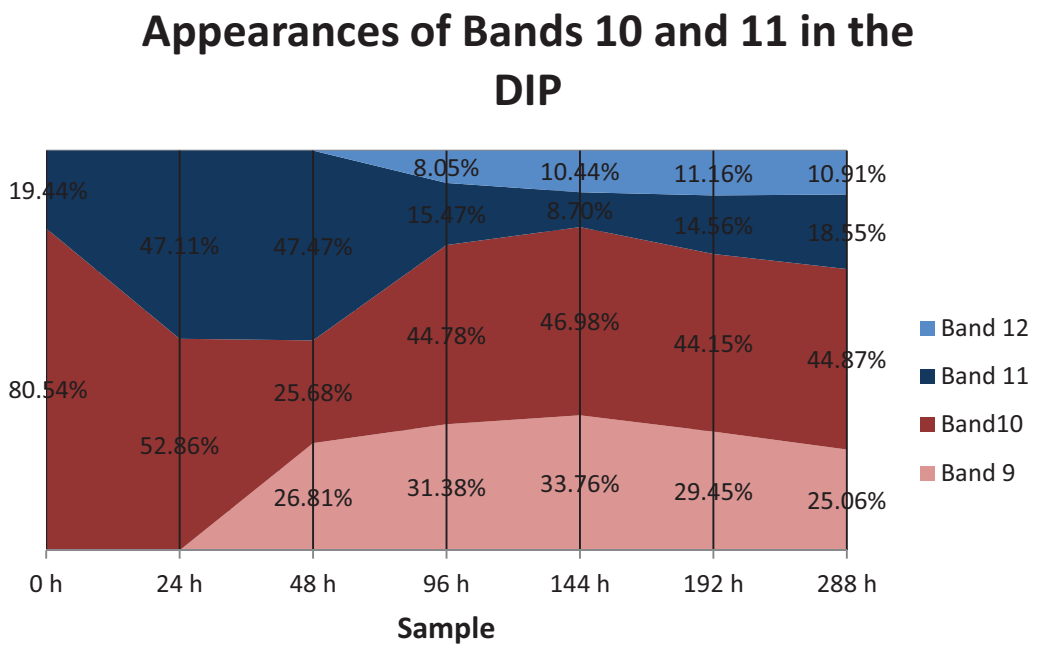

Fig. 13. Apprearances of Bands 10 and 11 in the DIP. Area chart focusing on the low molecular weight region of the protein profiles of the DIP samples, illustrating percentage-wise the appearance of bands 12 and 9.

4.3 LC-MS-MS Analysis

There were one doublet and three individual bands selected for LC-MS-MS analysis. These bands were selected because of their prominence and the unique changes that occur in them throughout the time course. The first sample selected (LS-MS-MS Sample 1) includes bands 2 and 3 from the 288 h DIP sample. These bands were dominated by different forms of myosin, and can therefore prove to be a good marker for normalization in the future, because it can be assumed to be expressed constitutively throughout the differentiation process. The second sample (LS-MS-MS Sample 2) selected includes band 6 from the 24 h DIP. Because of its molecular weight and dominance, it was thought to include actin. The results, however, indicate that this band had predominance (84.55%) of the protein vimentin. Vimentin is a part of the cytoskeleton, and has roles involving cell adhesion (Ivaska, 2007). Therefore, this protein would be very typical in a detergent-soluble sample.

The third sample selected (LS-MS-MS Sample 3) included a band 7 from the 288 h DIP sample. This band was intriguing because the extreme changes in density that occurs in it through time course. The results show that the band is fairly diverse, with a majority of the content (22.65%) belonging to subunit 2 of the mitochondrial cytochrome b-c1 complex. This may be an indication of high metabolic activity occurring within the myotube at that stage of myogenesis, but it would seem this protein should be enriched in the DSP. The second greatest proportion (12.53%) of the peptide content was identified as vimentin, as in the second band. Because vimentin is localized to the cytoskeleton, this may explain the growing presence of the band in the DIP, and its decreasing presence in the DSP; if that band does indeed include similar protein content.

The final sample selected (LS-MS-MS Sample 4) was band 11 from the 24 h DIP sample. This may be a case of phospohorylation and dephosphorylation of various kinases detected in the sample may also contribute to these shifts as well. The largest percentage 56.91% belonged to Peptidyl-prolyl cis-trans isomerase A, which is suggestive of metabolic activity related to protein synthesis. This is similarly indicative of structural reorganization of the sarcomere and cytoskeleton during myogenesis.

4.4 Future Work

The analysis presented here has identified trends in particular bands selected from the protein profiles of differentiating C2C12 cultures harvested at set time points during the process of differentiation. A deeper analysis of these band trends could be gained through 2-dimensional gel electrophoresis analysis. The use of LS-MS-MS analysis provided us the identity and relative proportion of the proteins in four of the bands. A more

comprehensive analysis could further use LS-MS-MS to identify the protein content of the same bands selected as observed in samples of different time points. This could give a clear picture of expression changes that occur within differentiating C2C12 cells, particularly if it can be paired with quantitative real-time PCR (qrtPCR) to identify transcription levels relative to a constitutively expressed "housekeeping" gene. These data would provide a comprehensive overview of the proteome of this cell line.

Additional ongoing work is focused on the cytoskeletal proteome of C2C12 cells, and general morphological differences in the developing myotubes cultured on fascia. Theoretically, the presence of fascia would have widespread implications on cytoskeletal development, which can be tracked via electrophoretic analysis of the DSP. It will therefore be important to identify the protein content in bands of DSP samples, as well. The 1-dimensional analysis of the DSP provided by the research presented here did not show the obvious density changes that were observed in the DIP. All the bands, save for the ~45 kDa band (Fig. 11), were relatively consistent, with fluctuations being of apparently little significance. However, by using LS-MS-MS to compare bands of different time points we can determine if proportional changes have occurred in a band.

An important aspect of this research is that it demonstrates, within the scope of our laboratory, a novel approach for proteomic analysis. Densitometry analysis through Quantity One has been shown here to be a powerful technique that requires considerably less effort and resources than 2-dimensional analysis, which in some circumstances, could supplant that analytical technique entirely. Gel quantitation also seems to be a more reliable protein quantitation technique than the Bradford Assay. Furthermore, these

densitometry techniques can be applied to nucleotide electrophoresis as well, as the software has various nucleotide gel-specific applications.

5. References

1. Baylor, Stephen M; Hollingsworth, Stephen. "Intracellular calcium movements during excitation-contraction coupling in mammalian slow-twitch muscle fibers" The Journal of General Physiology 139 (2012): 261-272.

2. Davis, Jonathan; Tikunova, Svetlana B. "Ca^{2+} exchange with troponin C and cardiac muscle dynamics" Cardiovascular Research 77 (2008): 619-626.

3. Deries, Marianne; Gonçalves, André B; Vaz, Raquel; Martins Gabriel G; Rodrigues, Gabriela; Thorsteindóttir, Sólveig. "Extracellular Matrix Remodeling Accompanies Axial Muscle Development and Morphogenesis in the Mouse" Developmental Dynamics 24 (2012): 350-364.

4. Georgiadas, V; Stewart, H.J; Pollard, H.J; Tavsanoglu, Y; Prasad, R; Horwood, J; Deltour, L; Goldring, K; Poirer, F; Lawrence-Watt, DJ; Maatz, Henrike; Schulz, "Lack of galectin-1 results in defects in myoblast fusion and muscle regeneration." Developmental Dynamics 236 (2007): 1024-1024

5. Guo, Wei; Schafer, Sebastian; Greaser, Marion L. Radke, Michael H; Liss, Martin Govindarajan, Thirupugal; Maatz, Henrike; Schulz, Herbert; Li, Shijun; Parrish, Amanda M; Dauksaite, Vita; Vakeel, Padmanabhan; Klassen, Sabine; Gerull, Brenda; Thierfelder, Ludwig; Regitz-Zagrosek, Vera; Hacker, Timothy; Saupe, Kurt W; Dec, G. William; Ellinor, Patrick; MacRae, Calum A; Spallek, Bastian; Fisher, Robert; Perrot, Andreas; Özcelik, Cemil; Saar, Kathrin; Hubner, Norbert; Gotthardt, Michael . "*RBM20*, A gene for hereditary cardiomyopathy regulates titin splicing" Nature Medicine 18 (2012): 766-773

5. Harris, Brittany N; Li, Hongyan; Terry, Monica; Ferrari, Michael B. "Calcium Transients regulate Titin Organization During Myofibrillogenesis" Cell Motility and the Cytoskeleton 60 (2005): 129-139.

6. Hiroki Shoji; Deltour, Louise; Takanori Nakamura; Tajbakhsh, Shahragim; Poirier, François. "Expression Patterns and role of Galectin1 during early mouse myogenesis" Development Growth and Differentiation (2009): 608-615.

7. Ivaska, Johanna; Pallari, Hanna-Mari; Nevo, Jonna; Eriksson, John E. "Novel Functions of vimentin in cell adhesion, migration and signaling" Experimental Cell Research (2007): 2057-2062.

8. Knight, James DR; Kothary, Rashmi; "The myogenic kinome: protein kinases critical to mammalian skeletal myogenesis" Skeletal Muscle (2011) 1-29

9. Kontrogianni-Konstantopoulos, Aikaterini; Ackermann, Maegan A; Bowman, Amber L. Yap, Solomon V; Bloch, Robert J. "Muscle Giants: Molecular Scaffolds in Sarcomerogenesis" Physiological Reviews 89 (2009): 1217-1267.

8. Krüger, Martina; Linke, Wolfgang A. "The Giant Protein Titin: A Regulatory Node That Integrates Myocyte Signaling Pathways" The Journal of Biological Chemistry 286 (2011) 9905-9912

9. Linke, Wolfgang A; Krüger, Martina. "The Giant Protein Titin as an Integrator of Myocyte Signaling Pathways" Physiology 25 (2010) 186-198

10. Nocella, Marta; Colombini, Barbara; Bagni, Maria Angela; Bruton, Joeseph; Cecchi, Giovanni "Non-crossbridge calcium dependent stiffness in slow and fast skeletal

muscle fibres from mouse muscle" The Journal of Muscle Research and Cell Motility 32 (2012) 403-409

11. Sanger, Jean M; Sanger, Joseph W, "The Dynamic Z Bands of Striated Muscle Cells" Science Signaling 1 (2008) 1-3

12. Tagawa, Masashi; Ueyama, Tomomi; Ogata, Takehiro; Takehara, Naofumi; Nakajima, Norio; Isodono, Koji; Asada, Satoshi; Takahashi, Tomosaburo; Matsubara, Hiroaki; Oh, Hidemasa. "MURC a muscle restricted coiled-coil protein is involved in the regulation of skeletal myogenesis " American Journal of Physiology-Cell Physiology 295 (2008) 490-498

13. Thorsteindóttir, Sólveig; Deries, Marianne; Cachaço Ana Sofia; Bajanca, Fernanda. "The extracellular matrix dimension of skeletal muscle development" Developmental Biology 354 (2011) 191-207

14. Tskhovrebova, Larissa; Trinick, John "Roles of Titin in the Structure and Elasticity of the Sarcomere" Journal of Biomedicine and Biotechnology 2010 (2010) 1-7

15. Turnacioglu, Kenan K; Mittal, Balraj; Dabiri, Guissou A; Sanger, Jean M; Sanger, Joseph W. "An N-Terminal fragment of Titin Coupled to Green Fluorescent Protein Localizes to the Z-bands in Living Muscle Cells: Overexpression leads to myofibril disassembly" Molecular Biology of the Cell 8 (1997) 705-717.

16. Ullrich Nina D; Fischer, Dirk; Kornblum, Corneilia; Walter, Maggie C; Niggli, Ernst; Zorzato, Francesco; Treves, Susan. "Alterations of Excitation-Contraction Coupling and Excitation Couple Ca^{2+} Entry in Human Myotubes Carrying *CAV3* Mutations Linked to Rippling Muscle Disease" Human Mutation 32 (2010) 309-317

17. Vikhlyantsev, I.M; Podlubnaya Z.A. "On the Titin Isoforms" Biophysics 51 (2006) 842-848

18. Walker, Gary R; Watkins, Thomas; Ansevin, Carl F. "Identification of Autoantibodies Associated with Rippling Muscles and Myasthenia Gravis That Recognize Skeletal Muscle Proteins: Possible Relationships of Antigens and Stretch-Activated Ion Channels Biochemical and Biophysical Research Communications 264 (1999) 430-435

19. Watkins, Thomas C; Zelinka, Lisa M; Kesic, Matt; Ansevin, Carl F; Walker Gary R. "Identification of Skeletal Muscle Autoantigens by Expression Library Screening Using Sera From Autoimmune Rippling Muscle Disease (ARMD) Patients" Journal of Cellular Biochemistry 99 (2006) 79-87

20. Yokoyama, Shigetoshi; Asahara, Hiroshi. "The myogenic transcriptional network" Cellular and Molecular Life Sciences 68 (2011) 1843-1849

21. Zelinka, L; McCann S; Budde, J; Sethi, S; Guidos M; Giles, R;. Walker, G.R. "Characterization of the in vitro expressed autoimmune rippling muscle disease immunogenic domain of human titin encoded by TTN exons 248-249" Biochemical and Biophysical Research Communications 411 (2011) 501-505

Appendices

A1. Materials

Mammalian Cell Culturing	
Product	**Manufacturer**
C2C12 (ATCC® CRL-1772™)	American Type Culture Collection (ATCC) Manassas, VA
Dulbecco's Modification of Eagle's Media (DMEM)	Sigma-Aldrich Corporation St. Louis, MO
Fetal Bovine Serum (FBS)	American Type Culture Collection (ATCC) Manassas, VA
Penicillin-Streptomycin-Amphotericin Solution (PS)	MP Biomedicals, LLC Solon, OH
Trypsin	American Type Culture Collection (ATCC) Manassas, VA

Gel Electrophoresis	
Product	**Manufacturer**
Criterion TGX 8-16% 1mm Gel	Bio-Rad Laboratories Hercules, CA
Wide Range Protein Molecular Weight Standards	Amresco Corporation Solon, OH
Equipment	**Manufacturer**
Criterion Cell	Bio-Rad Laboratories Hercules, CA
Criterion Dodeca Cell	Bio-Rad Laboratories Hercules, CA
PowerPAC 3000	Bio-Rad Laboratories Hercules, CA

Gel Analysis	
Product	**Manufacturer**
Sypro Ruby Red	Bio-Rad Laboratories Hercules, CA
Equipment/Software	**Manufacturer**
Pharos FX Plus Molecular Imager	Bio-Rad Laboratories Hercules, CA
Quantity One 1-D Analysis Software	Bio-Rad Laboratories Hercules, CA

Miscellaneous Chemicals and Equipment	
Product	**Manufacturer**
acetone	Pharmco-AAPER Brookfield, CT
CHAPS	Sigma-Aldrich Corporation St. Louis, MO
Coomassie Brilliant Blue R-250	Fisher Scientific Pittsburgh, PA
dithiothreitol	Sigma-Aldrich Corporation St. Louis, MO
glacial acetic acid	Pharmco-AAPER Brookfield, CT
glycine	Amresco Corporation Solon, OH
hydrochloric acid	Pharmco-AAPER Brookfield, CT
magnesium chloride heptahydrate	Avantor Performance Materials Center Valley, PA
protease inhibitor tablet	Roche USA San Francisco, CA
RNeasy Mini Kit	Qiagen, Inc. Valencia, CA
sodium dodecyl sulfate (SDS)	Amresco Corporation Solon, OH
sucrose	Fisher Scientific Pittsburgh, PA
tris base	Fisher Scientific Pittsburgh, PA
Triton X-100	Sigma-Aldrich Corporation St. Louis, MO
urea	Amresco Corporation Solon, OH
Equipment	**Manufacturer**
DYNAC Centrifuge	Becton, Dickenson and Company Parsippany, NJ
Galaxy 16D Centrifuge	VWR International, LLC Radnor, PA
Olympus LH 50A Inverted Phase Contrast Microscope	Olympus America Center Valley, PA
SPOT Idea 5mp Mosaic	SPOT Imaging Solutions Sterling Heights, MI

A2. Solutions and Media

Media	Recipe
C2C12 Initial Growth Media (C2IGM)	79 ml DMEM 20 ml FBS 1 ml Penicillin-Streptomycin-Amphotericin Solution
C2C12 Growth Media (C2GM)	500 ml DMEM 55 ml FBS 5.5 ml Penicillin-Streptomycin-Amphotericin Solution
C2C12 Differentiation Media (C2GM)	500 ml DMEM 5.5 ml FBS 5.5 Penicillin-Streptomycin-Amphotericin Solution

Solution/Buffer	Recipe
Protein Solubilization Solution (PSS)	800 ml deionized water 24 g urea 385 mg dithiothreitol 2 g CHAPS
4X SDS PAGE Sample Buffer	12.5 g glycerol 0.76 g tris base 2.30 g SDS 12.3 ml 0.5 M hydrochloric acid 17.75 ml deionized water
Isotonic Wash Buffer	1.211 g tris base 0.406 g magnesium chloride heptahydrate 51.345 g sucrose 500 ml deionized water Adjust pH to 7.4
Triton X-100 Extraction Buffer	100 ml Isotonic Wash Buffer 0.5 ml Triton X-100 protease inhibitor tablet

Gel Electrophoresis and Analysis	
Buffer/Solution	**Recipe**
Tris-Glycine-SDS Running Buffer (TGS)	800 ml deionized water 30.2 g tris base 10.0 g SDS 188 glycine
Coomassie Stain	2.5 g Coomassie Brilliant Blue R-250 100 ml Glacial Acetic Acid 450 Methanol 450 ml H20
High Destain / Sypro Fixing Solution	100 ml glacial acetic acid 400 ml methanol 500 ml deionized water
Low Destain	100 ml glacial acetic acid 150 ml methanol 750 ml deionized water